Temperature and oxygen fugacity constraints on CK and R chondrites and implications for water and oxidation in the early solar system

K. Righter
NASA Johnson Space Center, Houston, Texas 77058, USA

K.E.Neff
Department of Geological Sciences, Indiana University, Bloomington, Indiana 47401, USA

For Journal of NIPR, September 2006
Revised January 2007

Abstract: Recent chondritic meteorite finds in Antarctica have included CB, CH, CK and R chondrites, the latter two of which are among the most oxidized materials found in meteorite collections. In this study we present petrographic and mineralogic data for a suite of CK and R chondrites, and compare to previous studies of CK and R, as well as some CV chondrites. In particular we focus on the opaque minerals – magnetite, chromite, sulfides, and metal – as well as unusual silicates – hornblende, biotite, and plagioclase. Several mineral thermometers and oxy-barometers are utilized to calculate temperatures and oxygen fugacities for these unusual meteorites compared to other more common chondrite groups. R and CK chondrites show lower equilibrium temperatures than ordinary chondrites, even though they are at similar petrologic grades (e.g., thermal type 6). Oxygen fugacity calculated for CV and R chondrites ranges from values near the iron-wustite (IW) oxygen buffer to near the fayalite-magnetite-quartz (FMQ) buffer. In comparison, the fO_2 recorded by ilmenite-magnetite pairs from CK chondrites are much higher, from FMQ+3.1 to FMQ+5.2. The latter values are the highest recorded for materials in meteorites, and place some constraints on the formation conditions of these magnetite-bearing chondrites. Differences between mineralogic and O isotopic compositions of CK and R chondrites suggest two different oxidation mechanisms, which may be due to high and low water:rock ratios during metamorphism, or to different fluid compositions, or both.

1. Introduction

Ordinary, enstatite, and carbonaceous chondrite groups define a solar nebula with distinct compositional characteristics that range from reduced (E) to oxidized (C), but mainly metal-bearing and for the most part dry. Chondritic meteorites define a continuum from reduced (all Fe as metal) to oxidized (all Fe oxidized into silicates and oxides), with only a few unusual types that deviate from this trend (e.g., Krot et al., 2003). Oxygen isotopes are correlated with the Mg# (Mg/(Mg+Fe) molar) of olivines and pyroxenes in chondrites (Rubin, 2005; Wasson et al., 2000), suggesting a link between oxidation and oxygen isotopes, but the details of the timing, mechanism and controlling equilibria remain controversial. Any role for water has been relegated to that introduced into and available in the matrix in the form of phyllosilicates such as serpentine and smectite (Brearley, 2006). Our understanding of the conditions prevailing in the early solar nebula have been enhanced by new chondrite groups such as the metal-rich and heavily shocked CB, the oxidized and metamorphosed CK, and the oxidized (and perhaps hydrous) R chondrites. These groups have been defined by meteorites found by both the Japanese and US Antarctic meteorite recovery programs (Table 1).

CK carbonaceous chondrites are named after the first observed fall in Karoonda, South Australia in 1930, and are the only major group of carbonaceous chondrites that exhibits thermal metamorphism, from types 4 to 6 (e.g., Noguchi, 1993). Other grouplets or samples exhibiting thermal metamorphism include the Coolidge-Loongana grouplet (type 4; Weckwerth and Weber, 1998; Noguchi, 1994), Allende with high temperature mineral assemblages (Brenker and Krot, 2004), and clasts within CM and CI chondrites recording high temperatures (Brearley and Jones, 1998). The CKs are largely defined by Antarctic and

southern hemisphere finds, and also display features of metamorphism such as silicate darkening, recrystallization and shock veins (Rubin, 1992; Tomeoka et al., 2001). Silicate darkening is created by small grains of pentlandite and magnetite forming inside silicates. Calcium aluminum inclusions (CAI) and Fe-Ni metal are rare. The most common chondrule texture is porphyritic consisting of 99% of chondrules in the CK group (Scott and Krot, 2003), but a few barred olivine chondrules also exist. Olivine rims around BO were found in this study and opaque rims are common. The CK chondrites are also more oxidized than many other groups, perhaps due to aqueous alteration.

CV carbonaceous chondrites are named after the observed fall of Vigarano and are classified as petrologic type 3 or unequilibrated. CV chondrites have two subgroups; oxidized and reduced (McSween, 1977; Krot et al., 1998a). The oxidized groups consist of the Bali and Allende type. CVs contain mostly porphyritic chondrules, but also have barred olivine, radial pyroxene, and cryptocrystalline chondrules. CAI's and FeNi metal are common in CVs compared to the CKs (Table 2).

Rumuruti (R) chondrites are oxidized as exemplified by their general lack of metal, and fayalitic and NiO-rich olivine. Although there are a few low grade 3 types (Bischoff, 2000; Imae and Zolensky, 2003), most are thermally metamorphosed up to grade 6 (Kallemeyn et al., 1996). Since the initial proposition of a separate group (Rubin and Kallemeyn, 1989; Weisberg et al., 1991), many R chondrites have been discovered, and they are represented by a diverse mineralogy such as graphite, chromite, magnetite, troilite, pyrrhotite, and pentlandite (Yanai et al., 1985). This diversity has recently been extended with the discovery of an R chondrite containing Ca-amphibole and biotite (Satterwhite, 2006).

This study examines the petrology and mineralogy of some recent CK, CV and R chondrites, focusing on the opaque minerals found in the meteorites and the constraints they provide on temperature and oxygen fugacity. The temperature and oxygen fugacity of the CK and CV chondrites can be compared in order to help define their formation history relative to the more common and traditional chondrite groups (E, O and C). In addition the relation between water and oxidation will be discussed in light of the new hydrous oxidized R chondrite.

2. Experimental Methods

The polished CK thin sections used in the study include; MET01149,11 (CK3), EET90007,11 (CK5), EET99430,5 (CK4), QUE99679,7 (CK4), QUE99680,8 (CK5), EET87860,15 (CK5-6), LEW87009,13 (CK6) and RBT03522,11 (CK5) from JSC and Maralinga (CK4). The polished CV3 thin sections include the oxidized Bali type, ALH85006,23, the oxidized Allende type; LEW86006,2, ALH84028,11 and ALHA81258,4 and the reduced type, QUE93429,5 from the JSC collection. The thin sections were studied on an optical microscope using transmitted and reflected light and the 5910LV JEOL Scanning Electron Microscope at JSC. Modal abundances were determined using SEM back scattered electron mosaic images of sections and referencing to an optical microscope. Automatic determination of modes is unsatisfactory because many of the phases occur in association with chondrules and also matrix; as a result, modal analysis of images was done using a grid and manually counting (Table 2).

The mineral composition data (Tables 3 to 5) was obtained using the NASA-JSC Cameca SX100 electron microprobe using natural and synthetic minerals as standards and

PAP reduction scheme for ZAF corrections (Pouchou and Pichoir, 1991). The microprobe was operated with a beam current of 20 nA and an accelerating voltage of 20kV. FeO and Fe_2O_3 in oxides (Table 4a-d) were recalculated from total iron using charge balance and stoichiometry constraints (Carmichael, 1967).

3. Petrography and mineralogy

3.1 CK chondrites

The matrix:chondrule ratios in the CKs in the study are similar to those reported previously. The published data on modal abundances for the CK group (Table 2) show the matrix is 75% and the chondrules are 15% for the CK group (Scott and Krot, 2003). The average matrix in this study of CKs is 71.2% and the average amount of chondrules is 13.9%. The suite of CK chondrites studied here also contains lower modal abundances of CAI's than the CV chondrites, and close to the number typically documented previously in CKs (e.g., Scott and Krot, 2003; Keller et al., 1992; Kurat et al., 2002). Silicate darkening, discussed in detail for CK's by Rubin (1992) was also observed in many of the sections studied here, and especially in LEW87009, where darkened veins clearly cut across the equilibrated texture of the meteorite (Fig. 1). The opaque assemblages are abundant (3.5 to 18 %; Table 1), and found throughout the matrix, spherical inside chondrules and in rims around chondrules (Fig. 2).

The opaque assemblages consist of sulfides, magnetite, and ilmenite, but no metal was found in these sections (Fig. 3; also see Rubin, 1993, and Geiger and Bischoff, 1994). Magnetite is the most abundant opaque mineral in CK chondrites, and is nearly pure Fe_3O_4, with only small amounts of minor elements such as Cr, Ti and Al (Table 4). Exsolution

lamellae of ilmenite between 5-10 μm (Fig. 4) and aluminous spinel (Fig. 5) were found in the magnetite of almost all of the CK chondrite section studied. Magnetite was not found in MET01149 (petrologic type 3) – only large ilmenite grains (up to 200-300 μm). Ilmenite was also found as discrete grains in LEW87009 (petrologic type 6), perhaps attributable to the hotter conditions of thermal metamorphism.

The sulfides in the CK chondrites primarily are Fe or Fe,Ni sulfides. The most prevalent sulfide is pentlandite $(Fe,Ni)_9S_8$ and is often found in association with magnetite in CK chondrites (Fig. 7; Table 5). The other sulfides are pyrite, pyrrhotite ($Fe_{(1-x)}S$) and troilite. Millerite, NiS, was not found in this study, but has been reported in Maralinga (Geiger and Bischoff, 1994; Noguchi, 1993). And Huber et al. (2006) report violarite, chalcopyrite and laurite in a suite of CK chondrites. One 2 μm grain of ehrlichmanite, OsS_2, was found in LEW87009 (Fig. 6). Other platinum group element minerals have been found such as an Os-, Ru- and S-bearing phase in Yamato 693 (Nakamura et al., 1993) and some CKs studied by Geiger and Bischoff (1994).

3.2 CV chondrites

FeNi metal is common in the CV thin sections, compared to its absence in the CK sections. Metal in volume percent of the CV group is 0-5% and <0.01% for the CK group (Scott and Krot, 2003). We found FeNi metal in every CV thin section we examined (Table 5). Sulfide compositions in CV chondrites generally fall into two groups based on the oxidized and reduced subgroups. The reduced subgroup has lower Ni-content sulfide and contains more metal. The oxidized subgroup contains higher Ni content sulfide (10 to 25 wt%), and little to no metal (Krot et al., 1995; McSween, 1977). The significance of any compositional differences between CK and CV sulfides (with respect to fO_2 or fS_2) is not

clear due to the possibility that they equilibrated under different sets of thermal conditions. Magnetite was less abundant in the CV sections, but found in both the oxidized and reduced subgroups. It is also nearly pure Fe_3O_4, similar to that found in CK chondrites, with only minor amounts of Cr, Al and Ti (Table 4d). Ilmenite was not found in any of the CV thin sections, nor has it been reported in previous studies (e.g., Krot et al., 1995, 1998a,b).

3.3 R chondrites

Opaque minerals in the R chondrite LAP 04840 include chromite (Table 4d), pentlandite, and pyrrhotite (Table 5; Fig. 8). The pentlandite is similar in its Ni and Co contents to pentlandites analyzed here from CK chondrites. The chromite is mostly Fe and Cr, with only small amounts of Ti, Al, and Mg, reflecting the magnetite and chromite components (Table 4d). LAP 04840 also contains calcic amphibole and plagioclase feldspar in contact and textural equilibrium (Fig. 9). Together with olivine, chromite and sulfide, these minerals meet at 120˚ grain boundaries (Fig. 9).

Compositional variation in calcic amphiboles and biotites is extensive due to coupled exchange involving 1+ (K, Na), 2+ (Mg, Fe, Mn, Ca), 3+ (Al, Cr, Fe) and 4+ (Ti, Si) cations (e.g., King et al., 1999; Righter et al., 2002). In addition, the hydroxyl site can be occupied by OH, F, Cl and O. Correlations between Ti+Al+Fe+Cr and [2-(OH+F+Cl)] in a suite of well characterized calcic amphiboles were demonstrated by King et al. (1999). In the absence of measurements of OH and O, one can utilize this correlation to estimate the amount of water in an amphibole. Using this approach, and assuming the iron is half Fe^{2+} and half Fe^{3+} (not unreasonable considering the moderate pleochroism that is likely caused by the presence of Fe^{3+} and an oxy-amphibole component), the LAP 04840 amphibole could contain 2.0 wt% H_2O. Lower water contents would fall off the correlation line. This high

value is also consistent with estimates of high H_2O made by McCanta et al. (2006). For comparison, this is significantly more H_2O than amphiboles from terrestrial mantle melt inclusions, and those from martian meteorites. A similar exercise can be carried out for the biotite, since correlations between Ti+Al+ Fe^{3+}+Cr and [2-(OH+F+Cl)] were demonstrated in a suite of well characterized biotites by Righter et al. (2002). Using the same approach, the LAP 04840 biotite can contain 3.5 wt% H_2O. Again, lower water contents would fall off the correlation line. This is consistent with the estimates of McCanta et al. (2006), and again more water compared to biotites from martian meteorites and similar to those measured in kimberlite phlogopites (Fig. 10).

4. Intensive parameters: temperature and oxygen fugacity

4.1 Temperature

Exsolution of ilmenite within magnetite has been found in CK thin sections. The oxygen fugacity and temperature for the magnetite and ilmenite pairs were calculated using the Fe, Ti thermometer/oxybarometer (Lindsley and Anderson, 1988; Sack and Ghiorso, 1991), based on the distribution of Ti between ilmenite and magnetite:

$$XFe_2TiO_4 + (1\text{-}X)Fe_3O_4 + 1/4O_2 = XFeTiO_3 + (3/2\text{-}X)Fe_2O_3.$$

ulvospinel-magnetite solid solution ilmenite-hematite solid solution

The calculated temperature range for CK chondrites is 300 to 658 °C (Fig. 11). Although Geiger and Bischoff (1994) estimated the temperatures for CKs in the range of 550 to 1000 °C, recalculation of temperature using the Sack and Ghiorso (1991) oxy-thermometer results in lower temperatures that are consistent with those calculated from analyses in Table 4. These lower temperatures are further supported by the presence of pentlandite, found in the

highest petrologic types of CK chondrites, and not stable at temperatures greater than 883 K (610°C) (Fig. 12; Craig, 1973). Also, Turnock and Eugster (1962) studied the $FeAl_2O_4$ – Fe_3O_4 system and found a large miscibility gap in this system between 500 to 600 °C (Fig. 13). This suggests that the exsolution of nearly pure $FeAl_2O_4$ from magnetite in many of the CKs of this study (Fig. 5 and Table 4c,d), occurred during equilibration at temperatures <600 °C.

Calcic amphibole and plagioclase feldspar are also present in terrestrial amphibolites and granites, and have formed the basis of a hornblende-plagioclase thermometer (e.g., Holland and Blundy, 1994), in which exchange between calcic hornblende and plagioclase feldspar is modeled:

$NaCa_2Mg_5(AlSi_3)Si_4O_{22}(OH)_2 + NaAlSi_3O_8 = Na(CaNa)Mg_5Si_8O_{22}(OH)_2 + CaAl_2Si_2O_8$

edenite albite richterite anorthite

This thermometer (equilibrium B of Holland and Blundy, 1994) is calibrated across a large temperature range, and is only weakly pressure dependent. Because the pressure in an asteroid is likely to be < 1 kb, any small pressure dependence of the thermometer will have only a minor effect on the calculated temperatures. Temperatures calculated for LAP 04840 using amphibole and plagioclase compositions measured here (Table 3), and the following the protocol for mineral formulae described by Holland and Blundy (1994) yields a temperature of 600 (±40) °C for this unusual chondrite.

Temperatures calculated for the CK and R chondrites of this study are compared to temperatures calculated in two recent studies of ordinary chondrites (Fig. 14). In both cases, the temperatures calculated for type 6 CK and R chondrites are much lower than those calculated for type 6 ordinary chondrites by Kessel et al. (2004) based on olivine-spinel

equilibrium, and Slater-Reynolds et al. (2005) based on two pyroxene thermometry. Although some of this discrepancy may be attributed to differences in thermometers used in the various studies, it may also indicate that opaque mineral assemblages record lower metamorphic re-equilibration temperatures in the type 6 oxidized chondrites.

4.2 Oxygen fugacity

Petrologic evidence for an oxidized formation of CK chondrites includes the absence of Fe, Ni metal and the abundance of magnetite (Geiger and Bischoff, 1994; Kallemeyn et al., 1991). In addition, unusual sulfides, tellurides and alloys are present in CK chondrites (Geiger and Bischoff, 1991, 1994; Neff and Righter, 2006; Nakamura et al., 1993), as well as disturbed siderophile element patterns (low Re, Pd, Pt Ni and Se) compared to other carbonaceous groups (Koiwa and Ebihara, 2006; Huber et al., 2006; Horan et al., 2003); both of these features may be attributed to the oxidized nature of CKs. The CV chondrites contain FeNi metal in the reduced and oxidized subgroups (Krot et al., 1998a); even the oxidized CV's are more reduced than the CK chondrites since they contain metal.

Oxygen fugacities recorded by coexisting magnetite-ilmenite pairs in the CK chondrites studied here, range from $\log fO_2$ = -15 (950 K) to -30 (600 K). These values are more meaningful if they are compared to the values of a common buffer such as fayalite-magnetite-quartz (FMQ) at the same temperature. When this is done, the values for the CK chondrites range from 2.0 to 5.1 log fO_2 units above the FMQ buffer (Fig. 15). The CK temperature and oxygen fugacities plot in a linear trend, suggesting they equilibrated across a small range of temperature, but parallel to an oxygen buffer.

The CV thin sections in this study did not contain ilmenite, but analyses of the Fe, Ni metal (Table 5) can be used with magnetite compositions (Table 4) to place constraints on

oxygen fugacity using thermodynamic equilibria between metal and magnetite, $3Fe + 2O_2 = Fe_3O_4$. Oxygen fugacity can be calculated using thermodynamic data (Robie and Hemingway, 1995) and activity-composition relations (Sack and Ghiorso, 1991; Schwartzendruber et al., 1991) for magnetite and metal:

$\Delta G = -RT\ln K$, which upon rearranging yields: $fO_2 = \sqrt{\frac{a_{Fe3O4}^{spinel} e^{-\Delta G/RT}}{(a_{Fe}^{metal})^3}}$.

Because temperature cannot be calculated for the CV chondrites, oxygen fugacity was calculated across a temperature range of 300 to 900 °C for each metal composition, thus allowing a comparison to the T-fO_2 calculations for the CK chondrites. The results are shown in a graph of oxygen fugacity vs. temperature (Figure 11), are in agreement with calculations for the CV3s Yamato-86721 (Murakami and Ikeda, 1994) and Allende (Blum et al., 1988), and altogether indicate a more reduced nature for CV3's relative to CK chondrites.

Estimation of oxygen fugacity for R chondrites is possible by evaluation of several equilibria such as:

$$Fe + FeSiO_3 + 0.5\ O_2 = Fe_2SiO_4$$

metal pyroxene gas olivine

and

$$3FeSiO_3 + Fe_3O_4 = 3Fe_2SiO_4 + 0.5\ O_2.$$

pyroxene magnetite olivine gas

because R chondrites can contain metal, chromite, pyroxene and/or olivine (e.g., Bischoff et al., 1994). Using mineral compositions from Table 3 and 5, together with those from the literature (Bischoff et al., 1994; Kallemeyn et al., 1996; Rubin and Kallemeyn, 1994; Schulze et al., 1994; Weisberg et al., 1991), and activity models cited above as well as those of Wiser and Wood (1991) for olivine, and Sack and Ghiorso (1994) for pyroxene, we have calculated

oxygen fugacities for a suite of R chondrites. Values calculated can again be normalized to the FMQ buffer as done above for the CK and CV chondrites, and range from FQM-3.5 to FMQ (Fig. 15).

All three of these groups define oxygen fugacities higher than those of ordinary chondrites, as expected. R chondrites overlap with fO_2 values calculated for the Moon and Mars (Fig. 15). CV chondrites overlap with R chondrites, but are shifted to slightly higher fO_2. And the CK chondrites record the highest relative fO_2, well above the FMQ buffer. The average ΔFMQ for a CV in this study is -2.4 while the average ΔFMQ for CK is ~4.0. Although the general progression in oxidation from R to CV to CK holds, it is noted that there are some occurrences of very oxidized clasts in CV3 chondrites (Krot et al., 1998a, 1998b, 2006).

5. Discussion

5.1 Are CV and CK related?

The CV and CK carbonaceous chondrite groups have been compared to each other often because of petrographic similarities, and overlapping oxygen isotopic ratios. Some have suggested the two groups of carbonaceous chondrites formed from the same parent body and CKs are equilibrated CV chondrites (Greenwood et al., 2003, 2004). The oxidized CV group has been most closely related to CKs.

One large difference between the CK and CV chondrite groups is the degree of oxidation. Oxygen fugacities calculated in this study for CK chondrites are always higher than those for CVs – as much as 4 or 5 logfO_2 units higher. This suggests that if CKs were derived from CVs, the metamorphic conditions or fluids were very oxidizing. However,

there is petrographic evidence against a connection between CV and CK chondrites. About 50% of chondrules in CV chondrites are surrounded by coarse-grained rims. Even low grade CK4 chondrites should retain such rims, but they are only very rare in CK4s such as Karoonda (Kallemeyn et al., 1991).

Oxygen isotopic measurements of magnetite and olivine in CK chondrites (Clayton and Mayeda, 1999), yield nearly identical $\Delta^{17}O$ values, and lower than (more negative) those measured in CV chondrites. If magnetites in CK chondrites formed by oxidation involving the same kind of high $\Delta^{17}O$ water that formed many other magnetites in chondrites, they would be expected to have higher $\Delta^{17}O$ values. This suggests that if CKs were oxidized by the same water-bearing reservoir that oxidized many other chondrites (e.g., Wasson, 2000), they did not form from CV, because their $\Delta^{17}O$ are too low (negative).

Among equilibrated chondrites, there is a systematic change in olivine composition with oxidation, with reduced chondrites (EH and EL) having Fo-rich olivines (Fo_{99-100}), ordinary chondrites (H, L, LL) having intermediate Fo-contents (Fo_{70-86}), and R chondrites having the lowest Fo-contents (Fo_{60-63}). This progression can be understood in terms of increasing degree of oxidation of Fe-metal to form more FeO rich olivine (or pyroxene). Based on this trend, one might expect R chondrites, which have higher olivine Fe/Mg ratios to be more oxidized than CK chondrites, but the opposite is actually measured (CK olivines are ~Fo_{70}). This can be explained by oxidation in the presence or absence of FeNi metal (Fig. 16). At reduced conditions where metal is stable, olivine becomes more forsteritic with reduction as FeO is reduced to Fe (Nitsan, 1974). At more oxidized conditions where magnetite or hematite is stable (and FeNi metal is not) oxidation of FeO to Fe_2O_3 produces forsteritic olivine (Fig. 16). This is also true of terrestrial olivine-bearing igneous rocks,

where more oxidized samples have more Fo-rich olivine phenocrysts (e.g., Carmichael et al., 1996).

It is not unexpected that the metal-free equilibrated CK chondrites contain more forsteritic olivine than the metal-bearing R chondrites (Fig. 16B). It also suggests that the CK chondrites were metal-free (or nearly so) when oxidation began, rather than having lost metal during oxidation. CV chondrites with Fo_{90} olivine and little metal would make poor protoliths for CK chondrites, unless FeO was completely re-distributed (between chondrules and matrix) during metamorphism. But this would most likely erase the relict textures that we observe in CK5 and CK6 chondrites. For these reasons, it seems difficult to make CK chondrites from a CV precursor, but this study places new constraints on the relationship between oxidation and ferromagnesian phases (olivine and pyroxene) if such a connection exists.

5.2 Water and chondrites

Magnetites in CV chondrites have been attributed to aqueous alteration on asteroid parent bodies (Krot et al., 1998a; Hutcheon et al., 1998). Magnetite in CK chondrites may have a similar origin, but the presence of the water-bearing phase is not as obvious in CK's as it is in CV's (Brearley, 2006). This is partly because the CK chondrites have been metamorphosed and thus it is not known whether there were phyllosilicates in the matrix. This is also true for the oxidized R chondrites. Wood and Hashimoto (1993) demonstrate that talc and biopyriboles cannot condense from a high temperature gas even at the most oxidized conditions. Therefore they must have formed from water or lower temperature hydrous minerals that were present in the matrix. Because many R chondrites are type 3.8 or higher, no phyllosilicates have been found. Despite their high matrix modes, it has

appeared as if R chondrites are relative dry. However, with the discovery of an amphibole-bearing R chondrite, this scenario must be revised.

Amphibole stability has been studied in basaltic or basic systems at low pressures (e.g., Spear, 1981; Liou et al., 1981). Given the temperature range calculated by hornblende-plagioclase thermometry above (~600 ˚C), and the phase equilibria presented by Liou et al. (1981) for the FMQ buffer, it is clear that this assemblage could be present at pressures as low as 0.5 kb. Another body for which we have estimates of interior pressure is the ureilite parent body, based on olivine-pyroxene-graphite-gas equilibria (Walker and Grove, 1993; Warren and Kallemeyn, 1992). These equilibria define pressures as high as 60 to 80 bar, somewhat lower than the estimates for LAP 04840. Nonetheless the low pressures (0.5 to 1 kb) are consistent with an origin from an asteroid sized body (r = 100 to 180 km), and not the high pressures that are possible on a larger planet.

Many hydrous phases have been found so far in chondritic meteorites, and the extension to near 600 ˚C with LAP 04840 pushes the limits to higher temperatures, but also defines a gap in an intermediate temperature range. Phyllosilicates are abundant and clearly equilibrated at lower temperatures near 25 ˚C. Some reports of higher temperature micas such as clintonite (Keller and Buseck, 1991) push this to higher temperatures (150 ˚C). And a few studies have reported amphiboles, biopyriboles, and talc in Allende, suggesting localized temperatures of as high as 540 ˚C (Krot et al., 1995; Brearley, 1997; Brearley, 2006). However, there is a large gap between 150 and 600 ˚C in hydrous mineralogy that may be expected. For example, minerals such as talc, chloritoid, smectite, epidote, and lawsonite may all have a stability field in a chondritic composition between 150 and 600 ˚C. The stability of low temperature hydrous silicates has really dominated thinking on aqueous

alteration, temperature and oxidation. Yet the discovery of these equilibrated higher temperature hydrous silicates invites many questions that are fundamental to our understanding of these processes. For example, it is commonly assumed that above 250 °C water will exist as a fluid or gas, rather than structurally bound in minerals. Evidence for this comes from fayalitic olivines that may form from dehydration of phyllosilicates or by precipitation from oxidized aqueous fluids (e.g., Krot et al., 1995; 1998a,b; 2004). Thermal models for asteroids show that temperatures can be much higher than 250 °C (Grimm and McSween, 1989; Ghosh et al., 2006), yet the only modelling that has been done at higher temperatures has involved simplified Ca- and K-free compositions (e.g., Ganguly and Saxena, 1989). Thus it is no surprise that antigorite and talc are the hydrous phases predicted to be stable above 500 °C.

5.3 Oxidized chondrites and the nature of the oxidant

Detailed oxygen isotopic studies of components in chondrites have revealed that magnetites frequently have higher $\Delta^{17}O$ values than olivines in the same chondrite. This has led to formation models involving high $\Delta^{17}O$ asteroidal water reacting with relatively low $\Delta^{17}O$ chondrule silicates (e.g., Clayton and Mayeda, 1984; Wasson, 2000; Choi et al., 1997, 1998, 2005; Choi and Wasson, 2003). The range of values measured in ordinary and carbonaceous chondrites has been explained by variable reaction between water and nebular silicates (e.g., Wasson, 2000). The details of this process remain controversial and dependent upon knowing the oxygen isotopic composition of the solar nebula, one of the primary goals of the Genesis mission (e.g., Clayton, 2002; Hashizume and Chaussidon, 2005; Ireland et al., 2006; Thiemans, 1999, 2006; Wiens et al., 1999; Yurimoto et al., 2006). The two distinct

groups of oxidized chondrites discussed here – CK and R chondrites – may place additional constraints on the extent and timing of water as an oxidant in the early solar system.

Because R chondrites show ancient ages, they may provide insights into nebular processes (Sugiura and Miyazaki, 2006; Jogo et al., 2006; Dixon et al., 2003; Buikin et al., 2006; Nagao et al., 1999; Bischoff et al., 1994). Constraints from R chondrites suggest nebular water (or oxidant water) is ~ 3 $\Delta^{17}O$ above the TFL (Greenwood et al., 2000). Water reservoirs are not well characterized for R chondrites because so few are unequilibrated and hydrous phases have not been reported. Therefore, the existence of a hydrous phase in LAP 04840 may offer an opportunity to better understand the O and H isotopic composition of the water and its location or source in the solar system (e.g., 4 AU for CM chondrites; Eiler and Kitchen, 2004). In contradistinction to R chondrites, oxygen isotopic measurements of magnetite and olivine in CK chondrites (Clayton and Mayeda, 1999), yield nearly identical $\Delta^{17}O$ values (olivine are even slightly more negative), and lower than (more negative) those measured in CV chondrites. If magnetites in CK chondrites formed by oxidation involving the same kind of high $\Delta^{17}O$ water that formed many other magnetites in chondrites, they would be expected to have higher $\Delta^{17}O$ values.

Our current understanding of hydration and oxidation is linked to porosity, reaction progress, and the water:rock ratio during aqueous alteration (Zolotov et al., 2006). These authors identified oxidation and hydration events that are de-coupled. This is particularly important in understanding the two oxidized chondrite groups, since R and CK chondrites seem to have very different oxidation histories. It seems likely that R chondrites experienced oxidation involving a high $\Delta^{17}O$ water-bearing reservoir, and high water:rock ratios. In comparison, CK chondrites experienced extreme oxidation, involving low water:rock ratios

(consistent with the oxygen isotope evidence). If this is true, it is clear that oxidation mechanisms existed in the early solar system that did not involve water as a major oxidant.

6. Summary and future

Future efforts to understand conditions of oxidation and metamorphism in the early solar system might focus on several areas. First, modelling of oxidation and hydration equilibria should be extended to higher temperatures (up to 600 °C), since there is now abundant evidence for such conditions in the meteorite record. Second, fluids of variable compositions should be considered, because there is evidence for Cl and F bearing systems. For example, one phase that is always present in association with the magnetite-sulfide assemblages in CK chondrites, is chlorapatite (Table 3 and also Rubin, 1993). In addition, CI-like clasts in the Tsukuba H5-6 chondrite contain fluorite and fluorapatite (Nakashima et al., 2003). It is possible that Cl- or F-bearing fluids could have had a significant role in the oxidation and metamorphism, and quite different in reactivity and composition from Cl- or F-poor fluids. Such fluids will not only have different reactivities, but will also promote the stability of a variety of different solid phases. Third, additional isotopic studies of the rapidly growing CK chondrite group may also yield new constraints on the nature of oxidants in the early solar system. Fourth, efforts should be made to explore asteroid IR spectra for known (from meteorites) and potential hydrous phases to help identify parent bodies for these unique and interesting samples. Although some have argued that the presence of water as a gas or fluid will eventually cause disaggregation of any asteroidal body as the fluid or gas pressure increases above the mechanical strength, these samples clearly have residual water that has stabilized in equilibria established in an intermediate temperature range. Fifth and

finally, although we have some understanding of amphibole and biotite phase equilibria in hydrous systems, it is dominated by terrestrial compositions such as amphibolites (basaltic) and granites, rather than chondrites; phase equilibria on these new and unusual compositions may be necessary for a complete understanding of the P-T-fO_2-fH_2O history.

Acknowledgements

We would like to thank reviewers A. Krot, A. Rubin, and T. Noguchi, for their helpful and constructive reviews, as well as A. Yamaguchi for efficient editorial handling. Also, M. Zolensky and L. Keller for their time and expertise with respect to these meteorites, and for generosity in loaning thin sections and resources. We would like to give a special thanks to Loan Le for assistance with electron microprobe analysis. The US Antarctic Meteorite Working Group approved allocation of the many thin sections studied. KR wishes to thank the NIPR for an invitation to speak about this topic in 2006 – it provided an opportunity to think about these interesting meteorites and discuss similarities and differences with the CK and R chondrites in the NIPR Antarctic Meteorite Collection. This research was supported by a NASA RTOP to K. Righter and a summer internship to K. Neff through the Lunar and Planetary Institute.

References

Bischoff, A. (2000): Mineralogical characterization of primitive, type-3 lithologies in Rumuruti chondrites. Met. Planet. Sci. 35, 699-706.

Bischoff, A., Geiger, T., Palme, H., Spettel, B., Schultz, L., Scherer, P., Loeken, T., Bland, P., Clayton, R.N., Mayeda, T.K., Herpers, U., Meltzow, B., Michel, R., and Dittrich-Hannen, B. (1994): Acfer 217 –A new member of the Rumuruti chondrite group (R). Meteoritics 29, 264-274.

Blum, J.D., Wasserburg, G.J., Hutcheon, I.D., Beckett, J.R., and Stolper, E.M. (1988): 'Domestic' origin of opaque assemblages in refractory inclusions in meteorites. Nature 331, 405-409.

Brearley, A.J. (1997): Disordered biopyriboles and talc in chondrules in the Allende meteorite: possible origins and formation conditions, Lunar Planet. Sci. XXVIII, 153-154.

Brearley, A.J. (2006): The Action of Water, In Meteorites and the Early Solar System II (D.S.Lauretta and H.Y. McSween, Jr., eds.), The University of Arizona Press, Tucson, 587-624.

Brearley, A.J. and Jones, R.H. (1998) Chondritic meteorites. In *Mineralogical Society of America Reviews in Mineralogy, Volume 36. Planetary Materials*. (Ed. J.J. Papike). 400pp.

Brenker, F.E. and Krot, A.N. (2004): Late-stage, high-temperature processing in the Allende meteorite: record from Ca,Fe-rich silicate rims around dark inclusions. Amer. Mineral. 89, 1280-1289.

Buikin, A.I., Trieloff, M., Korochantseva, E.V., Hopp, J., Berlin, J., Stoffler, D. (2006): High precision ^{40}Ar-^{39}Ar dating of different Rumuruti lithologies. Met. Planet. Sci. 40, #5088.

Carmichael I. S. E. (1967): Iron-titanium oxides and oxygen fugacity in volcanic rocks. J. Geophys. Res. 72, 4665-4687.

Carmichael I. S. E., Lange, R. A., Luhr, J.F. (1996): Quaternary minettes and associated volcanic rocks of Mascota, western Mexico: a consequence of plate extension above a subduction modified mantle wedge. Contrib. Mineral. Petrol. 124, 302-333.

Choi, B.-G. and Wasson, J.T. (2003): Microscale oxygen isotopic exchange and magnetite formation in the Ningqiang anomalous carbonaceous chondrite. Geochim. Cosmochim. Acta 67, 4655-4660.

Choi, B.-G., McKeegan, K.D., Leshin, L.A., and Wasson, J.T. (1997): Origin of magnetite in oxidized CV chondrites: in situ measurement of oxygen isotopic compositions of Allende magnetite and olivine. Earth Planet. Sci. Lett. 146, 337-349.

Choi, B.-G., McKeegan, K.D., Krot, A.N., and Wasson, J.T. (1998): Extreme oxygen isotope compositions in magnetite from unequilibrated ordinary chondrites. Nature 92, 577-579.

Choi, B.-G., Cosarinsky, M., and Wasson, J.T. (2005): Oxygen isotopes of secondary phases in unequilibrated chondrites: implications for the fluids/ices in the nebula and asteroids. Oxygen in the Earliest Solar system, Gatlinburg, Tennessee, #9013.

Clayton, R.N. (2002): Self-shielding in the solar nebula. Nature 415, 860-861.

Clayton, R.N. and Mayeda, T.K. (1984): The oxygen isotope record in Murchison and other carbonaceous chondrites. Earth Planet. Sci. Lett. 67, 151-161.

Clayton, R.N. and Mayeda, T.K. (1999): Oxygen isotope studies of carbonaceous chondrites. Geochim. Cosmochim. Acta 63, 2089-2104.

Craig J.R. (1973): Pyrite-pentlandite assemblages and other low temperature relations in the Fe-Ni-S system. Am. J. Sci., 273A, p 496-510.

Dixon, E.T., Bogard, D.D., and Garrison, D.H. (2003): ^{39}Ar-^{40}Ar chronology of R chondrites. Met. Planet. Sci. 38, 341-356.

Dyar, M.D., Mackwell, S.J., McGuire, A.V., Cross, L.R. and Robertson, J.D. (1993): Crystal chemistry of Fe^{3+} and H^{+} in mantle kaersutite: implications for mantel metasomatism. Amer. Mineral. 78, 968-979.

Eiler, J.M. and Kitchen, N. (2004): Hydrogen isotope evidence for the origin and evolution of the carbonaceous chondrites. Geochim. Cosmochim. Acta 68, 1395-1411.

Ganguly, J. and Saxena, S.K. (1989): Theoretical predictions of volatile bearing phases and volatile resources in some carbonaceous chondrites. In (B. Faughnan and G. Maryniak, eds.) Space Manufacturing 7: Space resources to improve life on Earth, American Inst. of Aeron. Astron., Washington DC, 97-108.

Geiger, T. and Bischoff, A. (1991): Exsolution of spinel and ilmenite in magnetites from type 4-5 carbonaceous chondrites – indications for metamorphic processes. Meteoritics 26, 337.

Geiger, T. and Bischoff, A. (1994): Formation of opaque minerals in CK chondrites. Planetary and Space Science 43, 485-498.

Ghiorso M. and Sack R.O. (1991): Fe-Ti oxide geothermometry: Thermodynamic formulation and the estimation of intensive variables in silicic magmas. Contrib. Mineral. Petrol. 108, 485-510.

Ghosh, A., Weidenschilling, S.J., McSween, H.Y., Jr., and Rubin, A.E. (2006): Asteroidal heating and thermal stratification of the asteroid belt. In (D.S. Lauretta and H.Y.

McSween, eds.) Meteorites and the Early Solar System, II. Univ. Arizona Press, Tucson, Arizona, 555-566.

Greenwood, J.P., Rubin, A.E., Wasson, J.T. (2000): Oxygen isotopes in R chondrite magnetite and olivine: links between R chondrites and ordinary chondrites. Geochim. Cosmochim. Acta 64, 3897-3911.

Greenwood, R.C., Kearsley, A.T., and Franchi, I.A. (2003): Are CK chondrites really a distinct group or just equilibrated CV's? 66th Annual Meteoritical Society Meeting, #5179.

Greenwood, R.C., Franchi, I.A. Kearsley, A.T., and Alard, O. (2004): The relationship between CK and CV chondrites: a single parent body source? LPSC XXXV, #1664.

Grimm, R.E. and McSween, H.Y., Jr. (1989): Water and the thermal evolution of carbonaceous chondrite parent bodies. Icarus 82, 244-280.

Hashizume, K. and Chaussidon, M. (2005): A non-terrestrial ^{16}O-rich isotopic composition for the protosolar nebula. Nature 434, 619-622.

Holland, T. and Blundy, J. (1994): Non-ideal interactions in calcic amphiboles and their bearing on amphibole-plagioclase thermometry. Contrib. Mineral. Petrol. 116, 433-447.

Horan M.F., R.J. Walker, J.W. Morgan, J.N. Grossman, A.E. Rubin (2003): Highly siderophile elements in chondrites. Chemical Geology 66, 4187-4201.

Huber, H., Rubin, A.E., Kallemeyn, G.W., and Wasson, J.T. (2006): Siderophile-element anomalies in CK carbonaceous chondrites: Implications for parent-body aqueous alteration and terrestrial weathering of sulfides Geochim. Cosmochim. Acta 70, 4019-4037.

Hutcheon, I.D., Krot, A.N., Keil, K., Phinney, D.L., and Scott, E.R.D. (1998): ^{53}Mn-^{53}Cr dating of fayalite formation in the CV3 chondrite Mokoia: evidence for asteroidal alteration. Science 282, 1865-1867.

Imae, N. and Zolensky, M.E. (2003): Mineralogical description of PRE 95404: A Rumuruti chondrite that includes a large unequilibrated clast. Met. Planet. Sci. 37, 5176.

Ireland, T.R., Holden, P., Norman, M.D., and Clarke, J. (2006): Isotopic enhancements of ^{17}O and ^{18}O from solar wind particles in the lunar regolith. Nature 440, 776-779.

Jogo, K., Shih, C.Y., Reese, Y.D., and Nyquist, L.E. (2006): ^{53}Mn-^{53}Cr systematics of Rchondrite NWA 753. LPSC XXXVII, #1518.

Kallemeyn, G.W., Rubin, A.E. and J.T.Wasson (1991): The compositional classification of chondrites: V. The Karoonda (CK) group of carbonaceous chondrites. Geochim. Cosmochim. Acta 55, 881-892.

Kallemeyn, G.W., Rubin, A.E. and J.T.Wasson (1996): The compositional classification of chondrites: VII. The R chondrite group. Geochim. Cosmochim. Acta 60, 2243-2256.

Keller, L.P. and Buseck, P.R. (1991): Calcic micas in the Allende Meteorite: evidence for hydration reactions in the early solar nebula. Science 252, 946-949.

Keller, L.P., Clark, J.C., Lewis, C.F., and Moore, C.B. (1992): Maralinga, a metamorphosed carbonaceous chondrite found in Australia. Meteoritics 27, 87-91.

Kessel, R., Beckett, J.R., Huss, G.R., and Stolper, E.M. (2004): The activity of chromite in multicomponent spinels: Implications for T-fO_2 conditions of equilibrated H chondrites. Met. Planet. Sci. 39, 1287-1305.

King, P.L., Hervig, R.L., Holloway, J.R., Vennemann, T., Righter, K. (1999): Oxy-substitution and dehydrogenation in mantle derived amphibole megacrysts. Geochim. Cosmochim. Acta 63, 3635-3651.

Koiwa, Y. and Ebihara, M. (2006): Possible terrestrial weathering effects on platinum group element abundances in Antarctic carbonaceous chondrites. Antarctic Meteorites XXX, NIPR, Tokyo, 40-41.

Krot, A.N., Scott, E.R.D., and Zolensky, M.E. (1995): Mineralogical and chemical modification of components in CV3 chondrites: nebular or asteroidal processing? Meteoritics 30, 748-766.

Krot, A.N., Petaev, M.I., Scott, E.R.D., Choi, B.-G., Zolensky, M.E., and Keil, K. (1998a): Progressive alteration in CV3 chondrites: more evidence for asteroidal alteration. Met. Planet. Sci. 33, 1065-1085.

Krot, A.N., Petaev, M.I., Zolensky, M.E., Keil, K., Scott, E.R.D., and Nakamura, K. (1998b): Secondary calcium-iron-rich minerals in the Bali-like and Allende-like oxidized CV3 chondrites and Allende dark inclusions. Met. Planet. Sci. 33, 623-645.

Krot, A. N., Keil, K., Goodrich, C. A., Scott, E. R. D. and Weisberg, M. K. (2003): Classification of Meteorites, In *Treatise on Geochemistry* (ed. A.M. Davis), volume 1: Meteorites, Comets and Planets, Elsevier Press, New York, p. 83-128.

Krot, A.N., Petaev, M.I., Bland, P.A. (2004): Multiple formation mechanisms of ferrous olivine in CV carbonaceous chondrites during fluid assisted metamorphism. Ant. Meteorite Res. 17, 153-171.

Krot, A.N., Hutcheon, I.D., Brearley, A.J., Pravdivtseva, O.V., Petaev, M.I., and Hohenberg, C.M. (2006): Timescales and settings for alteration of chondritic meteorites. In (D.

Lauretta and H.Y. McSween, eds), Meteorites and the early solar system II, University of Arizona Press, Tucson, 525-554.

Kurat, G., Zinner, E., and Brandstatter, F. (2002): A plagioclase-olivine-spinel-magnetite inclusion from Maralinga (CK): evidence for sequential condensation and solid-gas exchange. Geochim. Cosmochim. Acta 66, 2959-79.

Lindsley D.H. and Andersen D. J. (1988): Internally consistent solution models for Fe-Mg-Mn-Ti oxides: Fe-Ti oxides. Am. Min. 73, 714-726.

Liou, J.G., Kuniyoshi, S., and Ito, K. (1974): Experimental studies of the phase relations between greenschist and amphibolite in a basaltic system. Amer. Jour.. Sci. 274, 613-632.

McCanta, M. C., Treiman, A. H., Essene, E. (2006): LAP 04840: An Amphibole-bearing R Chondrite. Met. Planet. Sci. 41, A118.

McSween, H.Y., Jr. (1977): Petrographic variations among carbonaceous chondrites of the Vigarano type. Geochim. Cosmochim. Acta 41, 1777-1790.

Murakami, T. and Ikeda, Y. (1994): Petrology and mineralogy of Yamato86751 CV chondrite. Meteoritics 29, 397-408.

Nagao, K., Okazaki, R., Sawada, S., and Nakamura, K. (1999): Noble gases and K-Ar ages of five Rumuruti chondrites: Yamato Y-75302, Y-79182, Y-793575, Y-82002, and Asuka 881988, Antarctic Meteorite Research XXIII, 81.

Nakamura, T., Tomeoka, K., and Takeda, H. (1993): Mineralogy and petrology of the CK chondrites Yamato-82104, Yamato-693, and a Carlisle Lakes-type chondrite Yamato-82002. Proc. NIPR Symp. Antarct. Meteorites 6, 171-185.

Nakashima, D., Nakamura, T., and Noguchi, T. (2003) Formation history of CI-like phyllosilicate-rich clasts in the Tsukuba meteorite inferred from mineralogy and noble gas signatures. Earth Planet. Sci. Lett. 212, 321-336.

Neff, K. and Righter, K. (2006): Opaque mineral assemblages in the CK and CV carbonaceous chondrites. Lunar Planet. Sci. XXXVII, #1320.

Nitsan, U. (1974): Stability field of olivine with respect to oxidation and reduction. Jour. Geophys. Res. 79, 706-11.

Noguchi, T. (1993): Petrology and mineralogy of CK chondrites: implications for the metamorphism of the CK chondrite parent body. Proc. NIPR Symp. Antarct. Meteorites 6, 204-233.

Noguchi, T. (1994): Petrology and mineralogy of the Coolidge meteorite (CV4). Proc. NIPR Symp. Antarct. Meteorites 7, 42-72.

Pouchou, J.-L. and Pichoir, F. (1991): Quantitative analysis of homogeneous or stratified microvolumes applying the model "PAP". In Heinrich, K.F.J. and Newbury, D.E. (Eds.), Electron Microprobe Quantitation. Plenum Press, New York, 31-75.

Popp, R.K. and Bryndzia, L.T. (1992): Statistical analysis of Fe^{3+}, Ti, and OH in kaersutite from alkalic igneous rocks and mafic mantle xenoliths. Amer. Mineral. 77, 1250-1257.

Righter, K. and Carmichael, I.S.E. (1993): Mega-xenocrysts in alkali-olivine basalts: fragments of disrupted mantle assemblages. Amer. Mineral. 78, 1230-1245.

Righter, K., Dyar, M.D., Delaney, J.S., Vennemann, T.W., and R.L. Hervig (2002): Distribution of OH, O, Cl and F in biotite from volcanic rocks and correlations with octahedral cations. Amer. Mineral. 87, 142-153.

Righter, K., Drake, M.J., and Scott, E.R.D. (2006): Compositional relationships between meteorites and terrestrial planets. In Meteorites and the Early Solar System, II (ed. D. Lauretta and H.Y., Jr.), University of Arizona Press, Tucson, 803-828.

Robie, R. A. and Hemingway, B. S. (1995): Thermodynamic properties of minerals and related substances at 298.15 K and 1 Bar (10^5 Pascals) pressure and at higher temperatures. US Geological Survey Bulletin 2131, 465 pp.

Rubin, A.E. (1992): A shock-metamorphic model for silicate darkening and compositionally variable plagioclase in CK and ordinary chondrites. Geochim. Cosmochim. Acta 56, 1705-1714.

Rubin, A.E. (1993): Magnetite-sulfide chondrules and nodules in CK carbonaceous chondrites: implications for the timing of CK oxidation. Meteoritics 28, 130-135.

Rubin, A.E. (2005): Relationships among intrinsic properties of ordinary chondrites: oxidation state, bulk chemistry, oxygen-isotopic composition, petrologic type and chondrule size. Geochim. Cosmochim. Acta 69, 4907-4918.

Rubin, A.E. and Kallemeyn, G.W. (1989): Carlisle Lakes and Allan Hills 85151: members of a new chondrite grouplet. Geochim. Cosmochim. Acta 53, 3035-3044.

Rubin, A.E. and Kallemeyn, G.W. (1994): Pecora Escarpment 91002: a member of the new Rumuruti (R) chondrite group. Meteoritics 29, 255-264.

Sack, R.O. and Ghiorso, M. (1991): An internally consistent model for the thermodynamic properties of Fe-Mg-titanomagnetite-aluminate spinels. Contrib. Mineral. Petrol. 106, 474-505.

Sack R.O. and Ghiorso M.S. (1994): Thermodynamics of multicomponent pyroxenes I. Formulation of general model. Contrib. Mineral. Petrol. 116, 277-286.

Satterwhite, C. and Righter, K. (2006): Antarctic Meteorite Newsletter 29, no. 1.

Schulze, H., Bischoff, A., Palme, H., Spettel, B., Dreibus, G., and Otto, J. (1994): Mineralogy and Petrology of Rumuruti: the first meteorite fall of the new R chondrite group. Meteoritics 29, 275-286.

Scott, E.R.D. and Krot, A.N. (2003): Chondrites and their components. In *Treatise on Geochemistry* (ed. A.M. Davis), volume 1: Meteorites, Comets and Planets, Elsevier Press, New York, p. 143-200.

Schwartzendruber, L.J., Itkin, V.P., and Alcock, C.B. (1991): The Fe-Ni system In (P. Nash, ed.) Phase Diagrams of Binary Nickel Alloys. ASM International, Materials Part, OH, 110-132.

Slater-Reynolds, V. and McSween, H.Y., Jr. (2005): Peak metamorphic temperatures in type 6 ordinary chondrites: An evaluation of pyroxene and plagioclase geothermometry. Met. Planet. Sci. 40, 745-754.

Spear, F.S. (1981): An experimental study of hornblende stability and compositional variability in amphibolite. Amer. Jour. Sci. 281, 697-734.

Sugiura, N. and Miyazaki, A. (2006): Mn-Cr ages of Fe-rich olivine in two Rumuruti chondrites. Earth Planets Space 58, 689-694.

Thiemens, M.H. (1999): Mass-independent isotope effects in planetary atmospheres and the early solar system. Science 283, 341-345.

Thiemens, M.H. (2006): History and applications of mass-independent isotope effects. Ann. Rev. Earth Planet. Sci. 34, 217-262.

Tomeoka, K. et al. (2001): Silicate darkening in the Kobe CK chondrite: evidence for shock metamorphism at high temperature. Met. Planet. Sci. 36, 1535-1546.

Turnock, A.C. and Eugster, H.P. (1962): Fe-Al oxides: Phase relationships below 1000 C. Jour. Petrol. 3, 533-565.

Walker, D. and Grove, T.L. (1993): Ureilite smelting. Meteoritics 28, 629-636.

Warren, P.H. and Kallemeyn, G.W. (1992): Explosive volcanism and the graphite-oxygen fugacity buffer on the parent asteroid(s) of the ureilite meteorites. Icarus 100, 110-126.

Wasson, J.T. (2000): Oxygen-isotopic evolution of the solar nebula. Rev. Geophys. 38, 491-512.

Wasson, J.T., Kallemeyn, G.W., and Rubin, A.E. (2000): Chondrules in the LEW 85332 ungrouped carbonaceous chondrite: Fractionation processes in the solar nebula. Geochim. Cosmochim. Acta 64, 1279-1290.

Weckwerth, G. and Weber, D. (1998): Hammadah al Hamra 073, the third member of the Coolidge-type grouplet: implications for element fractionation trends in carbonaceous chondrites. Lunar Planet. Sci. XXIX, #1739.

Weisberg, M.K., Prinz, M., Kojima, H., Yanai, K., Clayton, R.N., and Mayeda, T.K. (1991): The Carlisle Lake-type chondrites: A new grouplet with high $\Delta^{17}O$, and evidence for nebular oxidation. Geochim. Cosmochim. Acta 55, 2657-2669.

Wiens, R.C., Huss, G.R., and Burnett, D.S. (1999): The solar oxygen-isotopic composition: predictions and implications for solar nebula processes. Met. Planet. Sci. 34, 99-108.

Wiser, N. M. and Wood, B.J. (1991): Experimental determination of activities in Fe-Mg olivine at 1400K. Contrib. Mineral. Petrol. 108, 146-153.

Wood, J.A. and Hashimoto, A. (1993): Mineral equilibrium in fractionated nebular systems. Geochim. Cosmochim. Acta 57, 2377-2388.

Yanai, K., Kojima, H., and Matsumoto, Y. (1985): A new type chondrite?: Yamato-75302 consists mostly of very high iron olivine. Meteoritics 20, 791.

Yurimoto, H., Kuramoto, K., Krot, A.N., Scott, E.R.D., Cuzzi, J.N., Thiemens, M.H., Lyons, J.R. (2007) Origin and evolution of oxygen isotopic compositions of the Solar System. In (B. Reipurth, D. Jewitt, K. Keil, eds), Protostars and Protoplanets V, University of Arizona Press, Tucson, 1-16.

Zolotov, M.Yu., Mironeneko, M.V., and Shock, E.L. (2006): Thermodynamic constraints on fayalite formation on parent bodies of chondrites. Met. Planet. Sci. 41, 1775-1796.

Table 1: CK, CV, and R chondrites from the US and NIPR collections.
[listed alphabetically by collection, and petrologic grade in parentheses following samples]

CK (97)	***CV (41)***	***R (25)***
ANSMET		
ALH 82135, 84038, 85002 (4)	ALH A81003, A81258	ALH 85151 (3.6)
DAV 92300 (4)	ALH 84028, 84037	PCA 91002, 91241 (3.8-6)
EET 99430 (4)	ALH 85006	LAP 02238, 03645 (?)
EET 83311 (5)	EET 92128	LAP 03639, 03731, 03793, 03902, 031387, 04845 (4)
EET 87860 (5/6)	EET 96010	LAP 031135, 031156 (4)
EET 87507 (+50 others; 5)	EET 96286	LAP 031144 (4)
GRA 98102 (4)	GRO 95652	LAP 031275 (5)
LAP 03834 (3)	LAP 02206, 02228	LAP 04840 (6)
LAP 03784 (5)	LAP 04843	PRE 95404, 95410, 95411, 95412 (3)
LAP 03923 (5)	LEW 86006	
LAP 031158 (5)	MAC 02528	
LAR 04317, 04318 (4)	MCY 05219	
LEW 87009 (6)	MET 00429, 00430	
LEW 87214, 87250 (4)	MET 00634, 00742, 00747, 00761	
LEW 86258 (4)	MET 01074, 01080	
MAC 02453 (5)	QUE 93429, 93639, 93744, 94688	
MCY 05232 (4)	QUE 94366, 94546	
MET 01149 (3)	QUE 97186	
MET 00739 (4)	RKP A80241	
PCA 91470 (4)	RBT 043021	
PCA 82500 (4/5)	TIL 91722	
QUE 99680, 99681 (5)		
QUE 99675-679 (4)		
QUE 93007 (5)		
RBT 03522 (5)		
NIPR		
A-87127 (6)	A-87344	Y-82002 (3.9)
A-880691 (4)	A-880835	Y-75302 (3.8)
A-880718 (5)	A-881317	A-881988 (4)
A-881277 (5)	Y-75260	Y-791827 (4)
A-881452 (6)	Y-791601	Y-793575 (3.8)
A-881473 (4)	Y-86009	
A-881725 (6)	Y-86751	
Y-693 (4/5)	Y-86752	
Y-82102, 82103, 82104, 82105 (5)		
Y-82191 (6)		

Table 2: Modal Abundance data (CV and CK groups from Scott and Krot, 2003).

meteorite	section	type	chondrules	opaques	CAIs	matrix
MET01149	11	CK3	25.0	7.0	2.0	66.0
EET99430	5	CK4	5.1	3.5	4.7	86.7
QUE99679	7	CK4	17.4	6.0	3.1	73.5
EET90007	11	CK5	19.1	7.5	8.7	64.7
QUE99680	8	CK5	24.0	18.3	n.d.	57.7
EET87860	15	CK5,6	6.9	11.8	10.7	70.7
LEW87009	13	CK6	0.0	4.0	n.d.	79.0
CK group			15	n.d.	4	75
CV group			45	n.d.	10	40

Table 3: Electron microprobe analyses of silicates

	LAP 04840		8			EET 90007	EET 99430	LEW 87009	MET 01149
Type	R					CK5	CK4	CK6	CK3
phase	plagioclase	olivine	hornblende	biotite	orthopyroxene	olivine	olivine	olivine	olivine
n	9	9	25	10	10	5	6	15	10
SiO_2	66.10	36.33	47.55	39.48	53.85	37.44	37.73	38.49	36.72
TiO_2	n.d.	0.00	0.52	0.91	0.02	0.02	0.02	0.01	0.01
Al_2O_3	22.23	0.07	7.34	13.44	0.14	0.05	0.03	0.05	0.02
Cr_2O_3	0.04	0.04	0.81	0.81	0.07	0.01	0.02	0.01	0.02
FeO	0.66	32.49	10.96	11.81	19.15	27.10	28.87	28.31	32.95
MnO	n.d.	0.43	0.14	0.05	0.40	0.26	0.24	0.24	0.39
NiO	-	-	-	-	-	0.41	0.60	0.54	0.06
MgO	n.d.	29.94	15.93	19.14	24.94	36.01	34.21	33.29	30.97
CaO	1.61	0.04	9.52	0.03	0.41	0.01	0.06	0.01	0.04
Na_2O	9.35	0.02	3.36	2.00	0.03	0.01	0.01	-	0.01
K_2O	0.26	n.d.	0.29	6.64	n.d.	-	-	-	-
F	-	-	0.11	0.13	-	-	-	-	-
Cl	-	-	0.05	0.11	-	-	-	-	-
Mg#	-	0.62	0.72	0.74	0.70	0.70	0.68	0.68	0.63
Total	100.36	99.44	96.47	94.45	99.07	101.35	101.81	100.96	101.20

n.d. = not detected

Table 4a: Electron microprobe analyses of oxide pairs from EET 87860 (CK5,6)

	ilm B	mag B	ilm A	mag A	ilm matrix	mag matrix	ilm C	mag C
SiO_2	0.11	0.12	0.13	0.10	0.10	0.09	0.15	0.12
TiO_2	40.72	0.55	46.59	0.35	42.92	0.70	29.00	0.46
Al_2O_3	4.97	0.99	4.59	0.89	7.04	1.24	7.07	0.42
Cr_2O_3	2.76	3.60	1.32	3.55	4.01	3.71	4.11	3.69
V_2O_3	0.17	0.10	0.19	0.08	0.18	0.10	0.15	0.11
FeO	46.82	85.97	43.26	86.26	42.30	85.66	53.89	87.04
MnO	0.80	0.03	0.93	0.03	0.86	0.04	0.74	0.03
NiO	0.30	0.32	0.14	0.25	0.04	0.23	0.17	0.18
ZnO	0.20	0.03	0.20	0.01	0.22	0.02	0.22	0.01
MgO	2.48	0.09	2.25	0.03	2.74	0.08	2.22	0.01
CaO	0.08	0.03	0.06	0.10	0.04	0.05	0.02	0.02
Na_2O	0.02	0.02	0.01	0.01	0.01	0.02	0.02	0.01
Total	99.42	91.85	99.67	91.65	100.44	91.93	97.76	92.09
FeO	30.95	0.08	36.70	0.00	32.70	0.27	21.15	0.30
Fe_2O_3	17.63	95.45	7.28	95.88	10.67	94.89	36.38	96.38
Recalc.	101.18	101.41	100.40	101.25	101.51	101.43	101.40	101.74
T °C	486		378		468		490	
Log fO_2	-20.07		-26.39		-21.72		-19.42	
Δ FMQ	+4.36		+3.64		+3.52		+4.83	

A, B and C are pairs analyzed from different areas in the same meteorite.
FeO, Fe_2O_3 are calculated according to charge balance and stoichiometry after Carmichael (1967).

Table 4b: Electron microprobe analyses of oxide pairs from QUE99679 (CK4)

	BO ilm	BO mag	BO2 ilm	BO2 mag	rim D ilm	rim D mag	grain G ilm	grain G mag
SiO_2	0.06	0.08	0.05	0.07	0.13	0.09	2.22	0.05
TiO_2	30.78	1.34	28.99	0.66	40.34	1.41	22.50	0.79
Al_2O_3	13.69	0.79	10.95	0.34	8.54	1.87	10.35	0.49
Cr_2O_3	4.53	3.45	4.15	3.53	4.00	3.49	3.23	3.35
V_2O_3	0.14	0.10	0.14	0.10	0.17	0.10	0.13	0.10
FeO	45.08	85.12	48.46	86.29	40.18	85.22	51.97	86.43
MnO	0.74	0.05	0.64	0.02	0.79	0.07	0.33	0.02
NiO	0.10	0.40	1.03	0.25	0.41	0.27	0.73	0.23
ZnO	0.34	0.01	0.31	0.03	0.23	0.05	0.24	0.02
MgO	3.70	0.11	3.24	0.02	3.33	0.13	3.38	0.11
CaO	0.04	0.04	0.35	0.15	0.02	0.01	1.59	0.06
Na_2O	0.03	0.01	0.03	0.01	0.01	0.01	0.06	0.01
Total	99.23	91.49	98.32	91.46	98.14	92.71	96.72	91.65
FeO	19.96	0.61	18.00	0.16	29.07	0.75	13.58	0.25
Fe_2O_3	27.91	93.92	33.84	95.71	12.34	93.86	42.66	95.77
Recalc.	102.02	100.90	101.71	101.05	99.38	102.10	100.99	101.24
T °C	654		543		564		581	
Log fO_2	-14.47		-17.57		-18.23		-16.33	
Δ FMQ	+3.94		+4.52		+3.09		+4.39	

BO and BO2 are analyses from a rim around a barred olivine chondrule; D and G are pairs analyzed from different areas in the same meteorite.
FeO, Fe_2O_3 are calculated according to charge balance and stoichiometry after Carmichael (1967).

Table 4c: Electron microprobe analyses of oxides from EET 99430 (CK4) and EET 90007 (CK5)

	EET99430						EET90007					
	mag A	ilm A	mag C	ilm C	mag E	ilm E	mag A	ilm A	mag BO	ilm BO	mag F	ilm F
SiO_2	0.15	0.03	0.06	0.07	0.17	0.14	0.04	0.07	0.06	0.07	0.07	0.11
TiO_2	0.40	37.56	1.53	31.25	0.27	18.54	0.81	42.60	0.28	18.33	0.73	37.70
Al_2O_3	0.63	8.19	0.60	8.10	0.39	9.53	0.98	5.91	0.46	9.23	0.50	7.24
Cr_2O_3	2.94	2.70	3.05	3.69	3.37	4.97	4.03	3.00	3.87	4.47	3.63	2.91
V_2O_3	0.11	0.12	0.12	0.13	0.14	0.13	0.11	0.15	0.10	0.12	0.10	0.14
FeO	82.44	38.80	86.13	49.91	86.96	61.97	85.44	43.33	86.93	60.18	86.27	44.18
MnO	0.00	0.46	0.01	0.38	0.00	0.22	0.01	0.61	0.00	0.23	0.00	0.52
NiO	0.33	0.05	0.16	0.09	0.21	0.12	0.25	0.45	0.25	0.18	0.21	0.17
ZnO	0.00	0.66	0.04	0.54	0.01	0.38	0.02	0.20	0.01	0.33	0.03	0.24
MgO	0.12	2.70	0.17	2.88	0.11	2.25	0.21	2.35	0.11	2.91	0.20	2.82
CaO	0.02	0.11	0.03	0.01	0.04	0.04	0.23	0.20	0.05	0.05	0.07	0.13
Na_2O	0.01	0.01	0.01	0.03	0.00	0.02	0.01	0.03	0.02	0.02	0.00	0.03
Total	87.14	91.37	91.89	97.08	91.67	98.30	92.13	98.90	92.13	96.11	91.82	96.20
FeO	0.00	27.77	0.92	22.08	0.00	12.11	0.00	32.72	0.00	10.62	0.05	27.92
Fe_2O_3	91.63	12.26	94.70	30.92	96.66	55.40	95.12	11.79	96.82	55.08	95.82	18.07
Recalc.	96.32	92.59	101.37	100.18	101.35	103.85	101.65	100.08	101.83	101.63	101.41	98.01
T °C	438		658		413		490		432		515	
Log fO_2	-22.23		-14.37		-22.91		-20.70		-21.98		-19.00	
Δ FMQ	+4.46		+3.92		+5.10		+3.55		+5.02		+4.20	

A, C, E in EET 99430 and ; A and F in EET90007 are pairs analyzed from different areas in the same meteorite; CO in EET90007 is a pair from a rim around a barred olivine chondrule.
FeO, Fe_2O_3 are calculated according to charge balance and stoichiometry after Carmichael (1967).

Table 4d: Electron microprobe analyses of oxides from various R, CV and CK chondrites

	LAP 04840	MET01149	LEW87009	QUE99680	QUE99680	EET99430
	R	CK3	CK6	CK5	CK5	CK4
	chromite	ilm	ilm	ilm	mag	spinel B
SiO_2	0.20	0.01	0.37	0.02	0.06	0.06
TiO_2	1.26	53.40	26.19	49.66	0.15	0.19
Al_2O_3	2.28	0.00	4.99	0.06	0.63	54.98
Cr_2O_3	18.50	0.12	3.28	0.20	3.30	7.06
V_2O_3	0.67	0.16	0.18	0.21	0.09	0.03
FeO	64.56	43.82	56.91	43.42	86.46	27.01
MnO	0.23	0.66	0.52	0.98	0.03	0.03
NiO	-	0.02	0.59	0.33	0.43	0.37
ZnO	-	0.00	0.32	0.01	0.00	2.91
MgO	1.63	1.89	2.43	1.59	0.06	10.64
CaO	1.21	0.04	0.03	1.40	0.22	0.01
Na_2O	-	0.00	0.00	0.01	0.01	0.08
Total	90.59	98.05	98.05	98.05	91.44	103.36
FeO		43.93	18.25	38.74	0.00	27.01
Fe_2O_3		0.00	42.96	5.20	96.08	0.00
Recalc.		98.03	102.35	98.57	101.06	103.36
T °C				302		
Log fO_2				-31.23		
Δ FMQ				+4.08		

FeO, Fe_2O_3 are calculated according to charge balance and stoichiometry after Carmichael (1967).

Table 5: Electron microprobe analyses of sulfides and metal

	LAP 04840 R	RBT 03522 CK	MET 01149 CK3 Rim	MET 01149 CK3 B	MET 01149 CK3 C	MET 01149 CK3 F	EET 90007 CK5 BO	LEW 87009 CK6	LEW 87009 CK6 Chalcopyrite	EET 87860 CK5,6	EET 87860 CK5,6 Chond	QUE 99679 CK4 F	QUE 93429 CV	QUE 93429 CV	ALH 84028 CV
Pentlandite															
Fe	30.66	30.46	-	32.67	36.89	39.88	32.92	36.55	42.21	25.61	29.03	30.88	-	-	-
Ni	33.63	32.07	-	33.05	29.42	26.14	27.59	21.08	0.54	38.46	38.04	30.50	-	-	-
Co	0.93	1.04	-	1.19	1.20	0.90	1.23	1.34	1.18	0.80	0.76	1.32	-	-	-
Cu	0.11	0.02	-	0.00	0.02	0.00	0.16	0.09	7.48	0.00	0.00	0.60	-	-	-
Zn	0.01	0.01	-	0.01	0.00	0.05	0.00	0.01	0.00	0.00	0.02	0.00	-	-	-
S	33.36	35.98	-	32.95	34.08	33.71	36.55	41.93	49.71	33.39	33.31	36.71	-	-	-
Total	98.73	99.62	-	99.89	101.62	100.68	98.52	100.99	101.11	98.27	101.22	100.06	-	-	-
FeS															
Fe	52.13	-	46.37	61.67	63.58	63.62	-	45.73		-	-	-	-	-	-
Ni	8.02	-	16.26	0.30	0.07	0.15	-	0.81		-	-	-	-	-	-
Co	0.32	-	0.90	0.00	0.00	0.00	-	1.31		-	-	-	-	-	-
Cu	0.13	-	0.07	0.00	0.01	0.03	-	0.21		-	-	-	-	-	-
Zn	0.02	-	0.00	0.01	0.00	0.03	-	0.00		-	-	-	-	-	-
S	37.98	-	36.19	38.21	37.26	36.43	-	53.44		-	-	-	-	-	-
Total	98.61	-	99.82	100.20	100.92	100.33	-	101.51		-	-	-	-	-	-
metal															
Fe	-	-	-	-	-	-	-			-	-	-	57.83	91.33	30.12
Ni	-	-	-	-	-	-	-			-	-	-	40.91	5.40	66.65
Co	-	-	-	-	-	-	-			-	-	-	0.82	2.98	1.84
Cu	-	-	-	-	-	-	-			-	-	-	0.18	0.00	0.07
Zn	-	-	-	-	-	-	-			-	-	-	0.00	0.01	0.00
S	-	-	-	-	-	-	-			-	-	-	0.01	0.00	0.02
Total	-	-	-	-	-	-	-			-	-	-	100.07	99.91	98.78

Figure Captions

Figure 1: Optical photomicrograph of LEW 87009. Height of sample is approximately 0.8 cm. Dark veins on the left side of the section illustrate the shock darkening present in this sample, and also many other CK chondrites (e.g., Rubin, 1992).

Figure 2: Back scattered electron (BSE) and optical photomicrograph images of a barred olivine chondrule surrounded by a rim of opaques from EET90007. Opaques are also present in the surrounding groundmass and as spherical assemblages within the recrystallized rim on the chondrule.

Figure 3: BSE mosaic images of the CK chondrite sections studied here, clockwise from upper left: MET 01149, QUE 99679, EET 99430, LEW 87009, EET 87860, and EET 90007. Each image consists of 50 to 100 individual images acquired in a systematic scanning grid, and has it own specific scale bar. These images allow one to assess the modal abundance and distribution of opaque minerals relatively quickly.

Figure 4: Two BSE images of magnetite grains containing exsolution lamellae of ilmenite from EET99430 and EET 90007. Width of lamellae is up to 10 μm.

Figure 5: BSE images of magnetite grains containing exsolution lamellae of hercynitic spinel in QUE 99680 and RBT 03522. These lamellae are irregular in shape compared to ilmenite, and are often tapered across a short distance. However, they are also generally thicker than the ilmenite lamellae.

Figure 6: BSE image of an erlichmannite (OsS_2) grain found in LEW 87009. It is found in association with pentlandite and chalcopyrite. Scale bar is 1 μm.

Figure 7: BSE image of a magnetite – pentlandite intergrowth from LEW87009. These typically form around other coarser grains or chondrules, and also in association with chlorapatite and pyrrhotite.

Figure 8: BSE image and optical photomicrograph of large opaque assemblage in the R chondrite LAP 04840. Main minerals are pentlandite, pyrrhotite, and chromite, but also present are calcic amphibole and biotite.

Figure 9: Higher magnification BSE image of calcic amphibole, plagioclase, chromite, olivine and sulfides in LAP 04840. Note the 120 ˚ triple junction grain boundaries, indicating textural equilibration of these phases.

Figure 10A: Correlations between Ti+Cr+Fe^{3+}+Al and (OH+F) for fully characterized terrestrial calcic amphiboles (from King et al., 1999; Righter and Carmichael, 1993; Dyar et al., 1993; Popp and Bryndzia, 1992) compared to the range defined by LAP 04840 assuming Fe is present in either 50% or 100% Fe_2O_3, and an estimated water content of 2.0 wt%. Water contents that are lower than 2 wt% will fall below the correlation line. Also shown for comparison are the relatively low OH contents of martian amphiboles (references from King et al., 1999). **Figure 10B**: Correlations between Ti+Cr+Fe^{3+}+Al and (OH+F) for fully characterized terrestrial biotites (from Righter et al., 2002) compared to the composition of biotite in LAP 04840, and assuming a water content of 3.5 wt%. Again, shown for comparison are the relatively low OH contents of martian biotites (references from Righter et al., 2002).

Figure 11: logfO_2 vs. inverse temperature (10^4/T(K)) calculated using ilmenite-magnetite pairs in CK chondrites, and logfO_2 calculated as a function of temperature for metal-magnetite pairs in CV chondrites (Table 4 and 5). Open circles are from analyses of oxide pairs reported by Noguchi (1993) and Geiger and Bischoff (1994), and closed circles are from this study (Table 4). Note that CKs are always approximately 4 logfO_2 units more oxidized than CVs.

Figure 12: Phase diagrams for the Fe-Ni-S system at 400 ˚C and 600 ˚C (from Craig, 1973). Top panel shows the composition of pentlandite and FeS from CK chondrites in this study and those reported by Geiger and Bischoff (1994).

Figure 13: Phase diagram for the Fe_3O_4-$FeAl_2O_4$ (magnetite-hercynite) system (Turnock and Eugster, 1962). The nearly pure magnetite and hercynite (< 5 mole % in each) found in several CK chondrites (Fig. 5), demonstrates that these samples equilibrated at temperatures no higher than 500 ˚C.

Figure 14: Histogram of temperatures calculated for CK and R chondrites from this study, compared to those calculated for equilibrated ordinary chondrites from the studies of Kessel et al. (2004) and Slater-Reynolds and McSween (2006). Even the type 6 CK and R chondrites do not record temperatures as high as the type 6 OC chondrites.

Figure 15: Histogram of relative oxygen fugacity (relative to the fayalite-magnetite-quartz buffer, or FMQ), for the R, CV and CK chondrites in this study, compared to other chondrite groups such as H, L, LL, and E (the latter from Righter et al., 2006). The large range of relative oxygen fugacities in chondritic materials starts at values similar to oxidized terrestrial magmas and extends down to approximately 10 logfO_2 units below the FMQ buffer. Vertical dashed line is the location of the iron-wustite oxygen buffer.

Figure 16A: Stability field of olivine in temperature – oxygen fugacity space (from Nitsan, 1974). At reducing conditions where Fe metal is stable, decreasing fO_2 produces more forsteritic olivine at FeO is reduced to Fe. At more oxidized conditions, where Fe metal is not stable, but magnetite is, increasing fO_2 also produces more fosteritic olivine, as FeO is oxidized to Fe_2O_3. Abbreviations are from the original paper and are: O = olivine, P = pyroxene, M = magnetite, W = wustite, S = silica. **Figure 16B:** A plot of relative oxygen fugacity vs. olivine composition (X_{Fo}) for a number of equilibrated chondrites (enstatite, ordinary, R, and CK chondrites). The trend from reduced E to oxidized R chondrites can be explained by progressive oxidation of FeNi metal. CK chondrites fall off of this trend at more forsteritic olivine compositions; this can be explained by oxidation in the absence of metal (see text for discussion). Fields for E, H, L, LL, and R chondrite groups are from data summarized in

Brearley and Jones (1998) and in Righter et al. (2006). Vertical hachured region is where metal breaks down during oxidation.

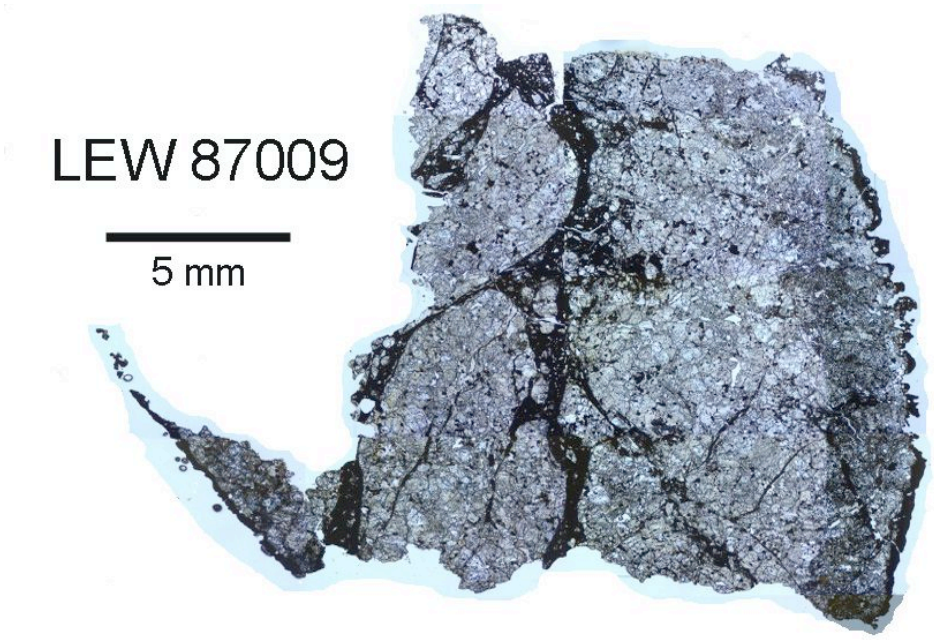

Figure 1.

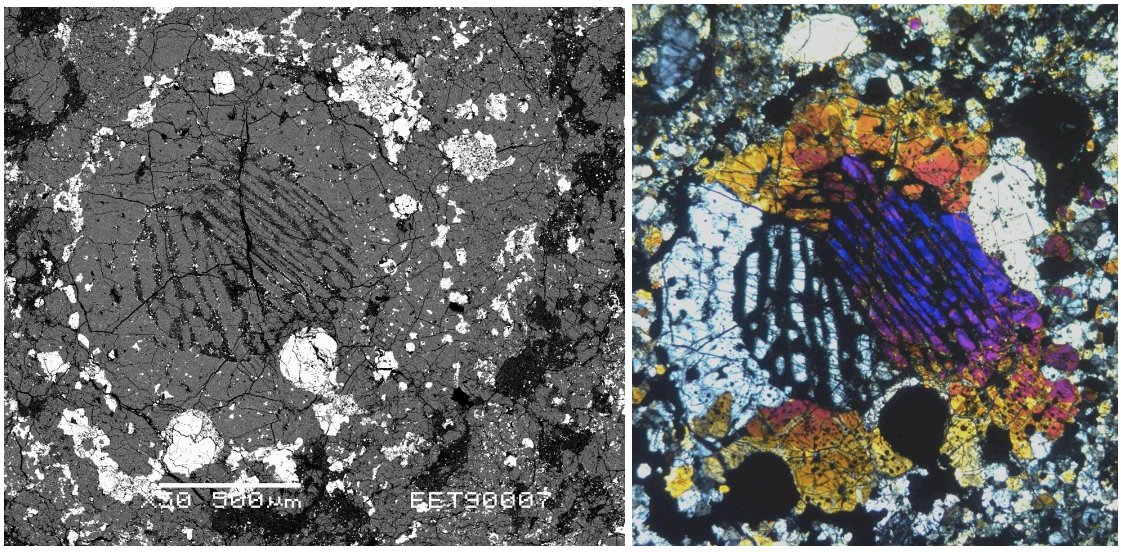

Figure 2.

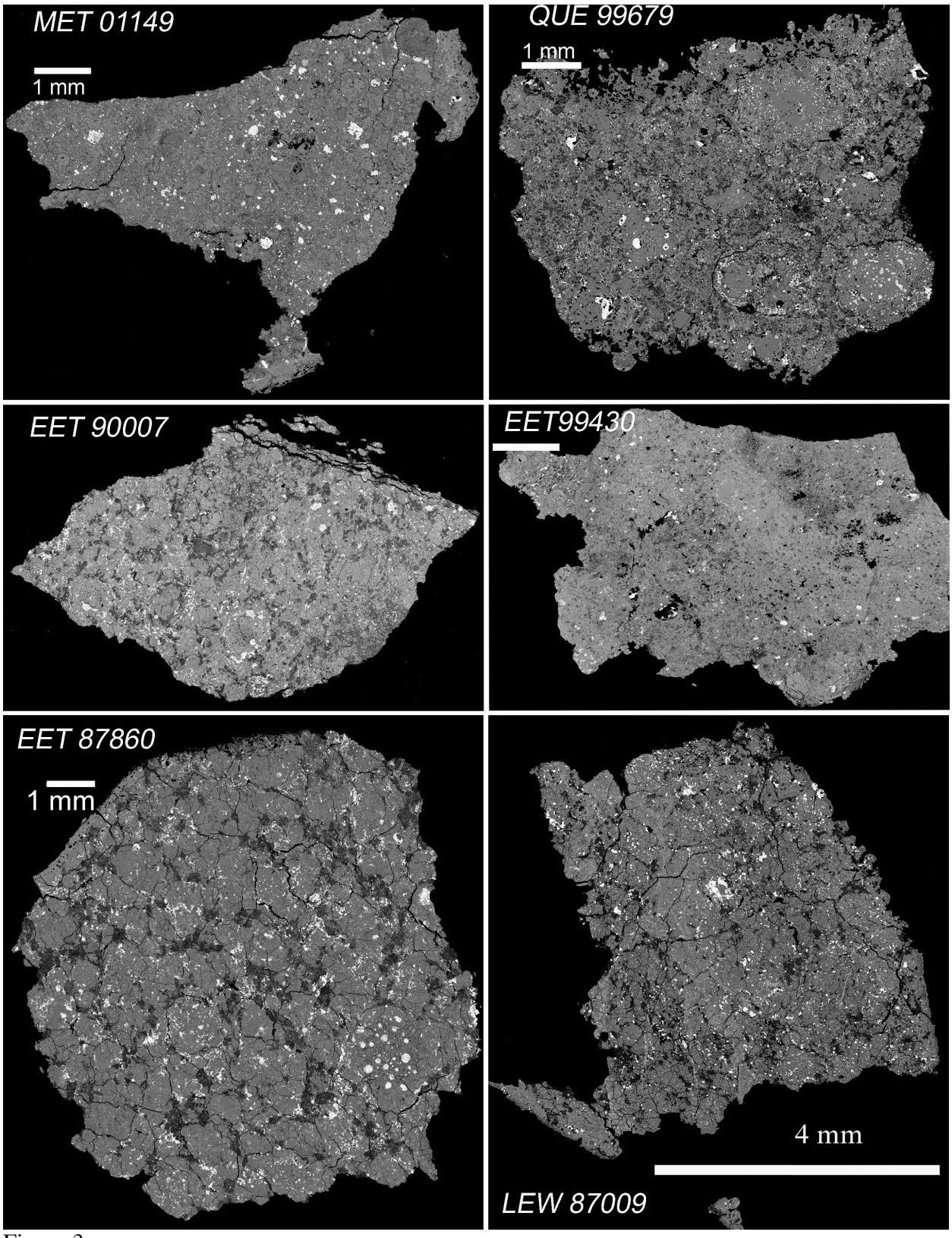
MET 01149
1 mm
QUE 99679
1 mm
EET 90007
EET99430
EET 87860
1 mm
4 mm
LEW 87009
Figure 3.

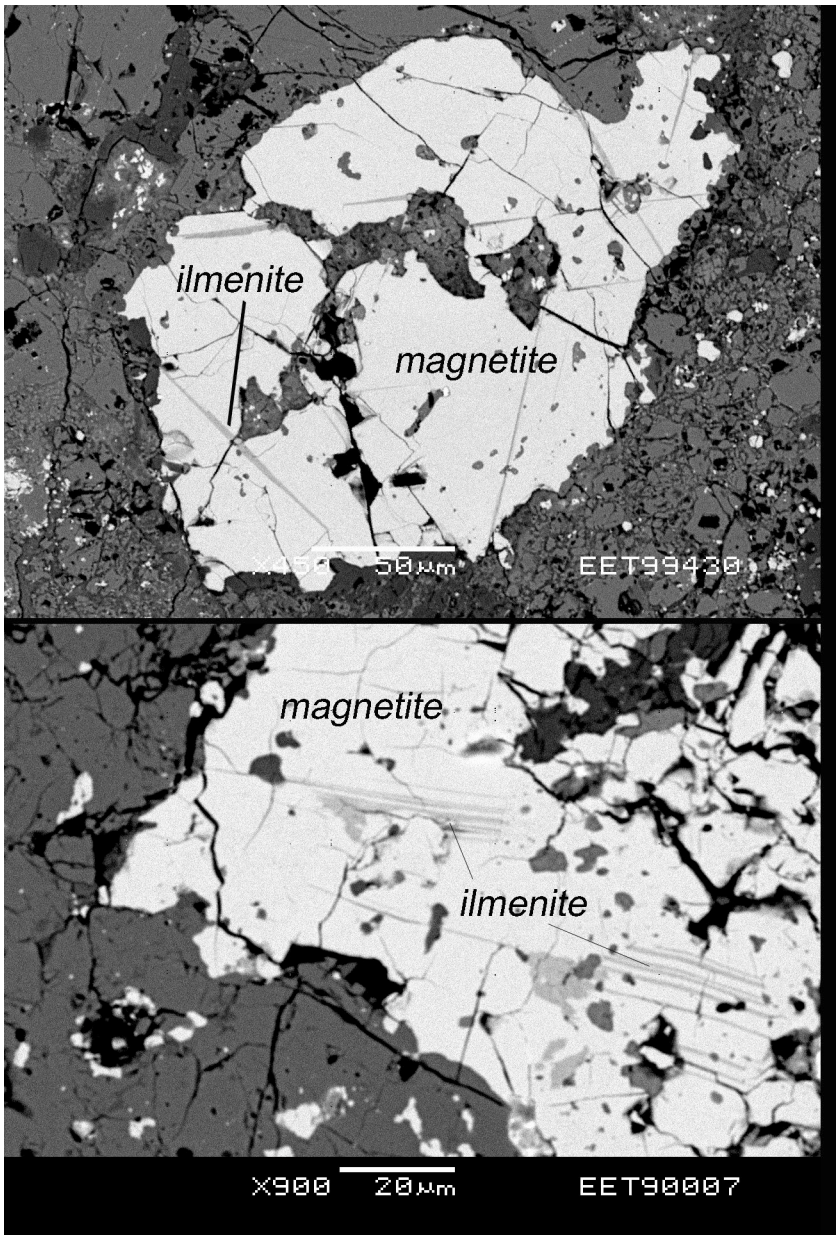
ilmenite
magnetite
50µm
EET99430
magnetite
ilmenite
X900
20µm
EET90007
Figure 4.

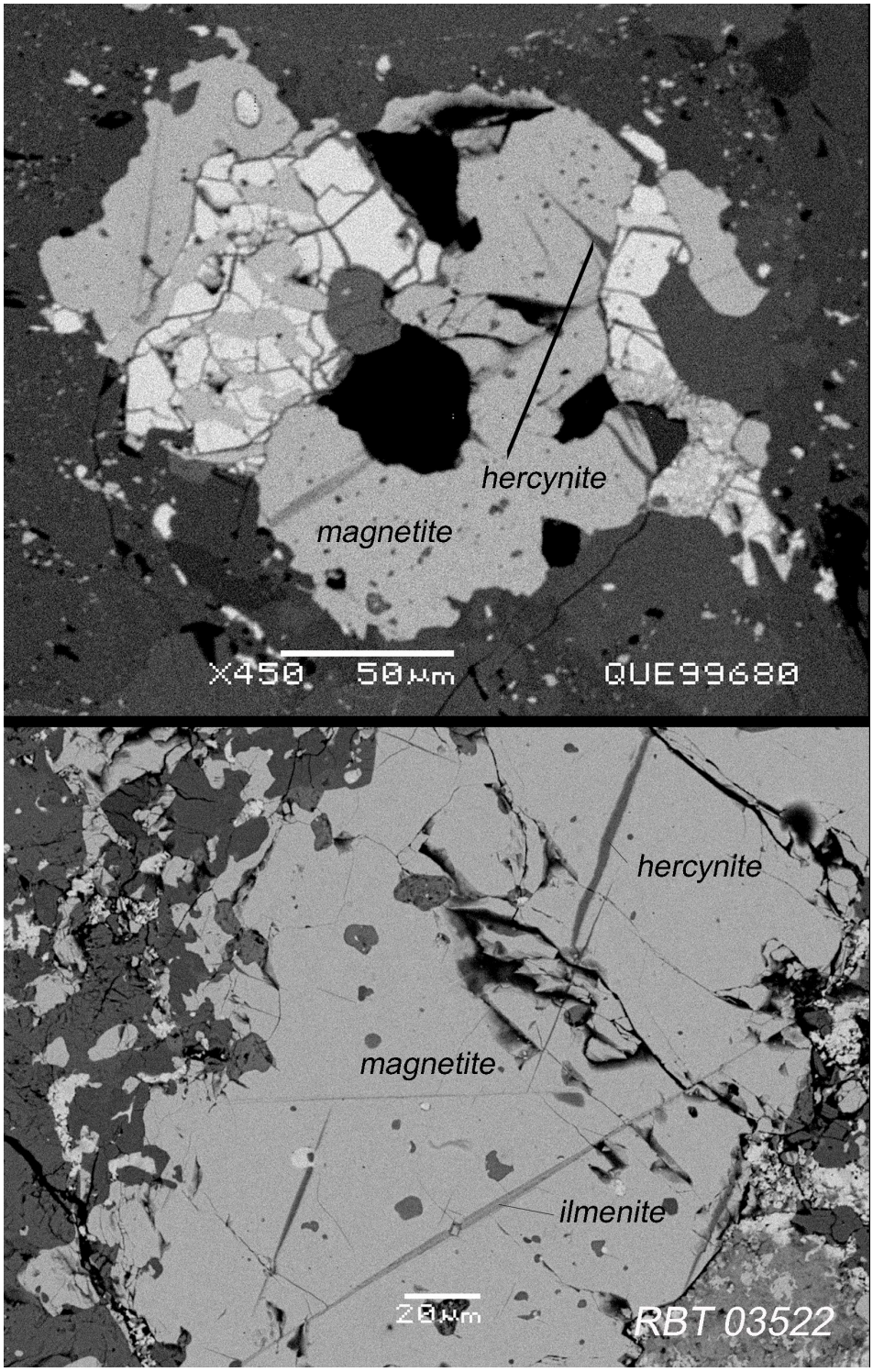
hercynite
magnetite
X450 50µm
QUE99680
hercynite
magnetite
ilmenite
20µm
RBT 03522
Figure 5.

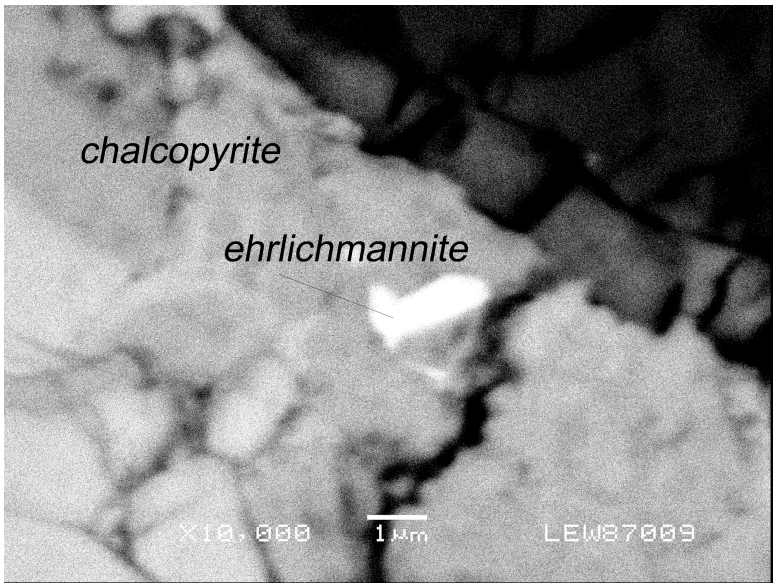

Figure 6.

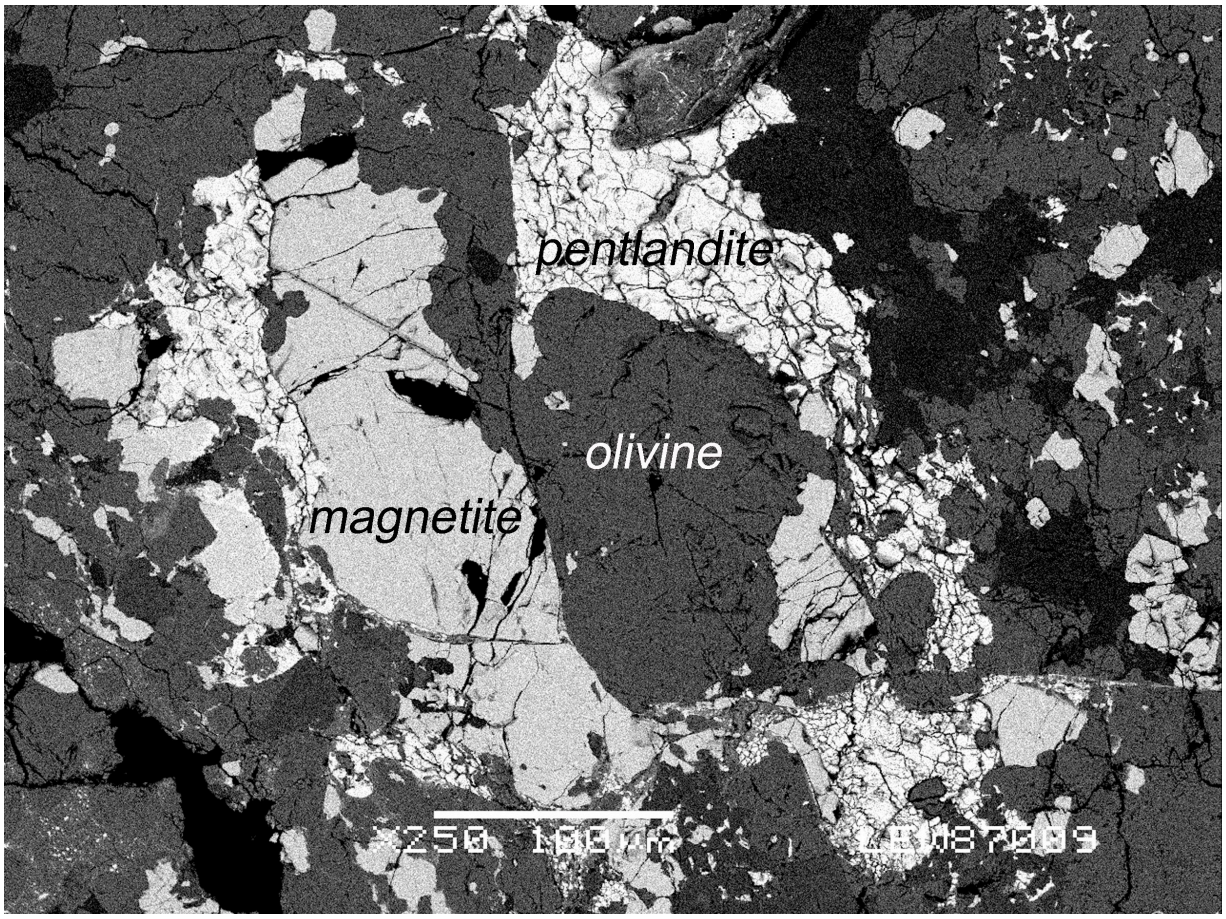

Fig. 7.

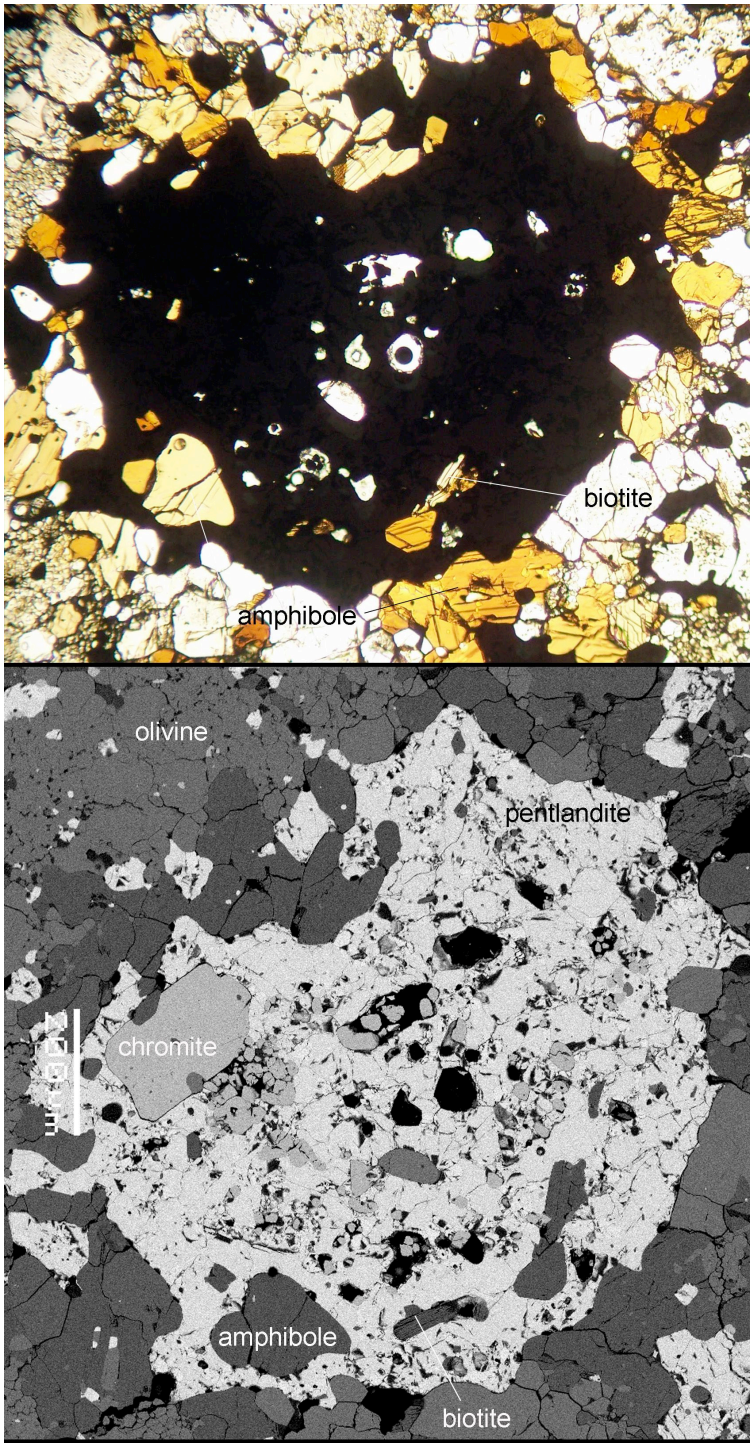
biotite
amphibole
olivine
pentlandite
chromite
1 mm
amphibole
biotite
Figure 8.

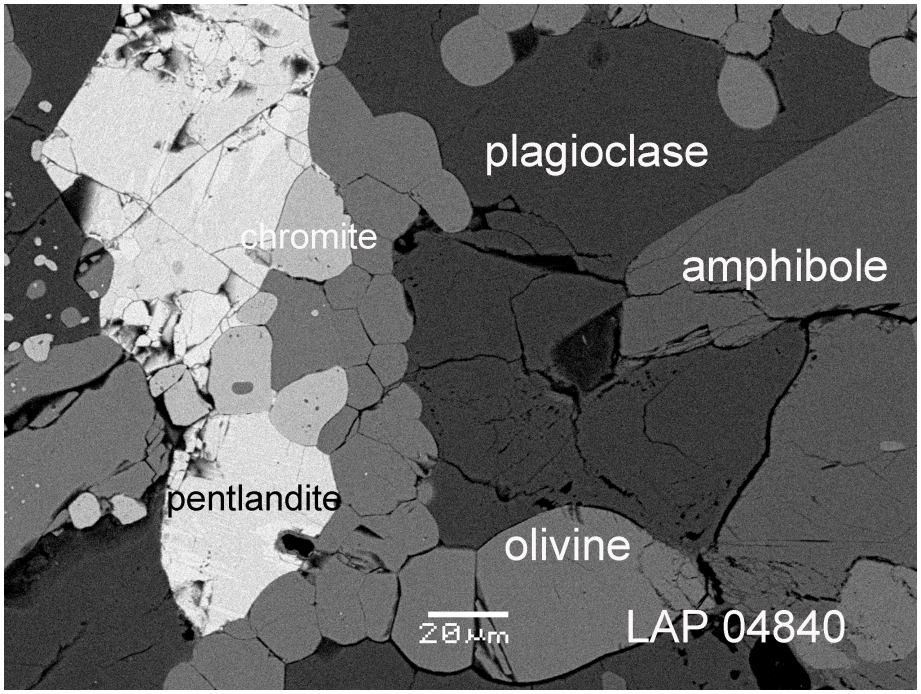
plagioclase
chromite
amphibole
pentlandite
olivine
20 µm
LAP 04840

Figure 9.

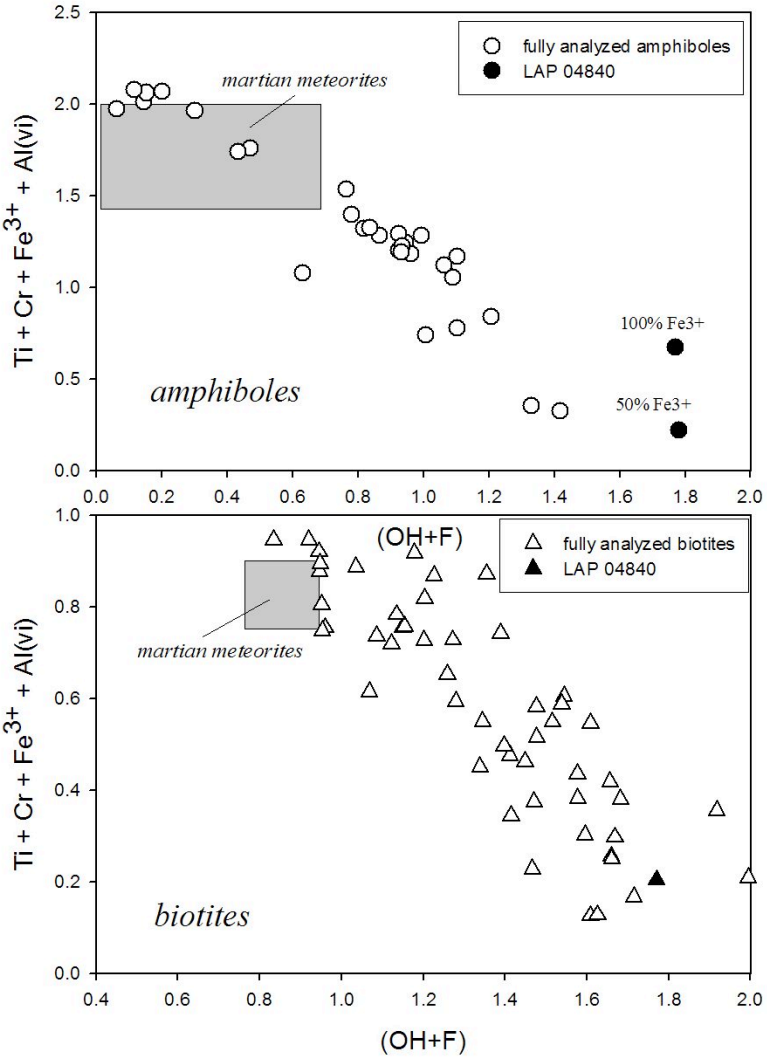
fully analyzed amphiboles
LAP 04840
martian meteorites
amphiboles
100% Fe3+
50% Fe3+
Ti + Cr + Fe3+ + Al(vi)
fully analyzed biotites
LAP 04840
martian meteorites
biotites
(OH+F)
(OH+F)

Figure 10.

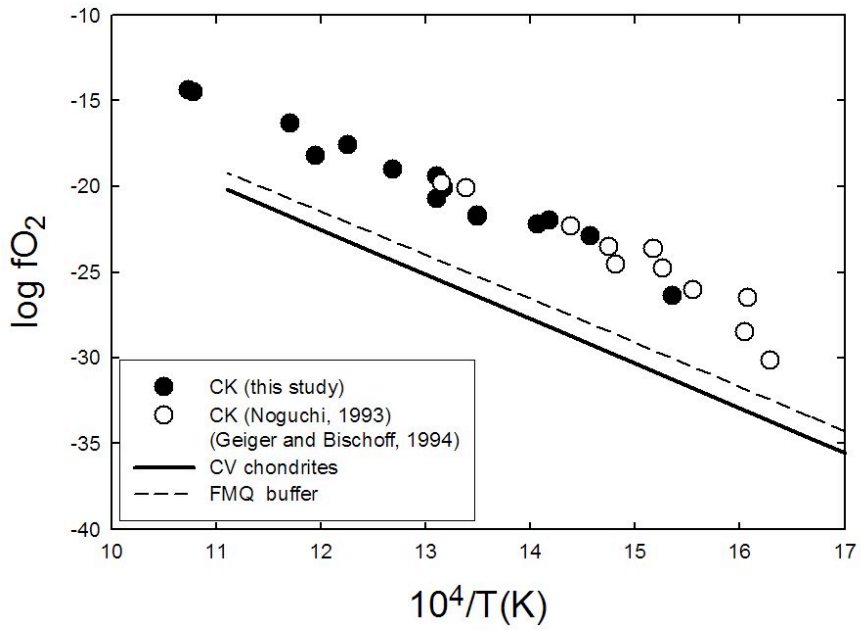
-10
-15
-20
-25
-30
-35
-40
log fO2
10
11
12
13
14
15
16
17
10^4/T(K)
CK (this study)
CK (Noguchi, 1993)
(Geiger and Bischoff, 1994)
CV chondrites
FMQ buffer

Figure 11.

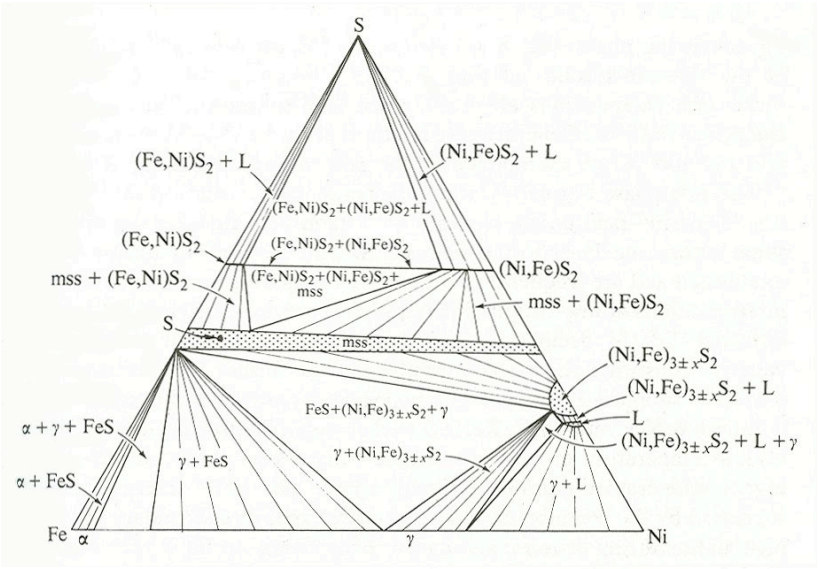
S
(Fe,Ni)S2 + L
(Ni,Fe)S2 + L
(Fe,Ni)S2+(Ni,Fe)S2+L
(Fe,Ni)S2
(Fe,Ni)S2+(Ni,Fe)S2
mss + (Fe,Ni)S2
(Fe,Ni)S2+(Ni,Fe)S2+ mss
(Ni,Fe)S2
mss + (Ni,Fe)S2
S
mss
(Ni,Fe)3±xS2
(Ni,Fe)3±xS2 + L
FeS+(Ni,Fe)3±xS2+γ
L
α + γ + FeS
γ + FeS
γ+(Ni,Fe)3±xS2
(Ni,Fe)3±xS2 + L + γ
α + FeS
γ + L
Fe
α
γ
Ni

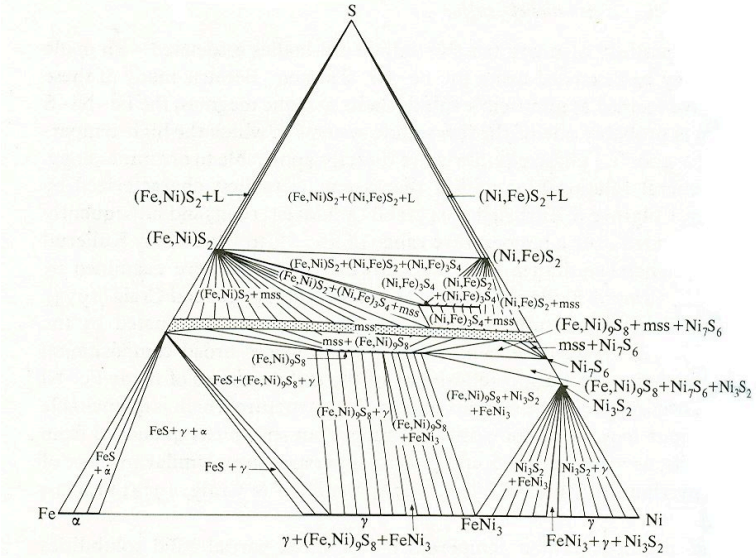
S
(Fe,Ni)S2+L
(Fe,Ni)S2+(Ni,Fe)S2+L
(Ni,Fe)S2+L
(Fe,Ni)S2
(Fe,Ni)S2+(Ni,Fe)S2+(Ni,Fe)3S4
(Ni,Fe)S2
(Ni,Fe)3S4
(Ni,Fe)S2+mss
(Fe,Ni)S2+mss
(Fe,Ni)S2+(Ni,Fe)3S4+mss
(Ni,Fe)3S4+mss
mss
(Fe,Ni)9S8+ mss +Ni7S6
mss+Ni7S6
mss + (Fe,Ni)9S8
(Fe,Ni)9S8
Ni7S6
FeS+(Fe,Ni)9S8+γ
(Fe,Ni)9S8+ Ni7S6+Ni3S2
(Fe,Ni)9S8+Ni3S2 +FeNi3
Ni3S2
(Fe,Ni)9S8+γ
FeS+γ+α
(Fe,Ni)9S8 +FeNi3
FeS +α
FeS + γ
Ni3S2 +FeNi3
Ni3S2+γ
Fe
α
γ
FeNi3
γ
Ni
γ+(Fe,Ni)9S8+FeNi3
FeNi3+γ+Ni3S2

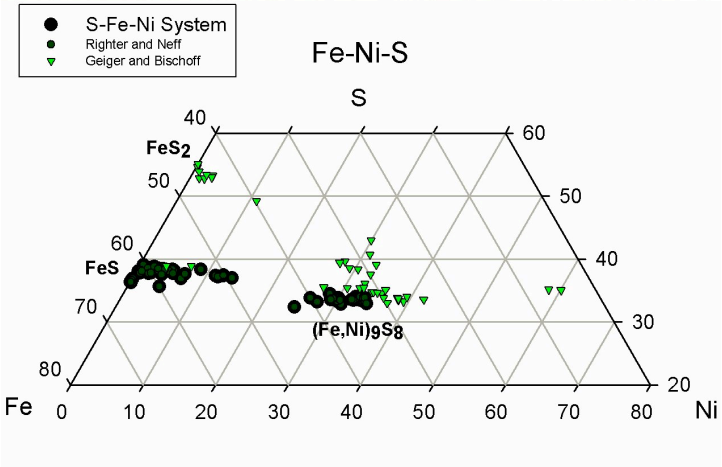
S-Fe-Ni System
Righter and Neff
Geiger and Bischoff
Fe-Ni-S
S
FeS2
FeS
(Fe,Ni)9S8
Fe
Ni
40
50
60
70
80
0
10
20
30
40
50
60
70
80
60
50
40
30
20

Figure 12.

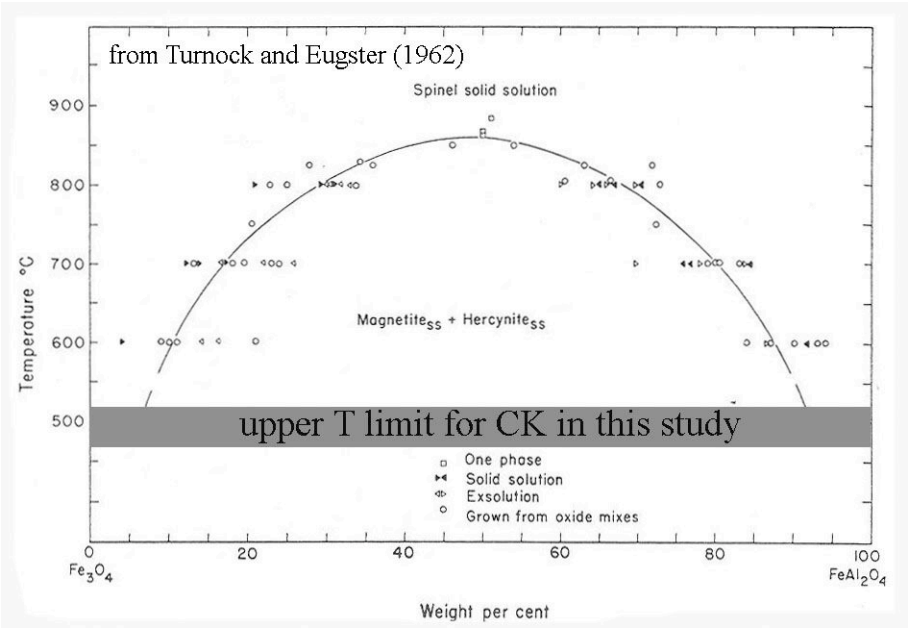
from Turnock and Eugster (1962)
Spinel solid solution
900
800
700
600
500
Temperature °C
Magnetite$_{ss}$ + Hercynite$_{ss}$
upper T limit for CK in this study
One phase
Solid solution
Exsolution
Grown from oxide mixes
0
20
40
60
80
100
Fe_3O_4
$FeAl_2O_4$
Weight per cent

Figure 13.

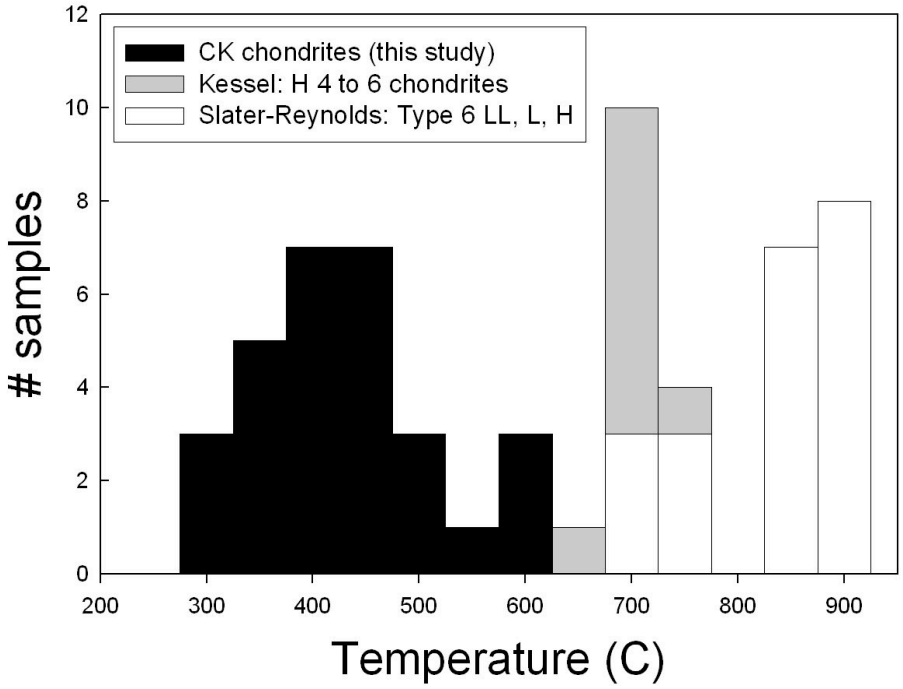
CK chondrites (this study)
Kessel: H 4 to 6 chondrites
Slater-Reynolds: Type 6 LL, L, H
samples
Temperature (C)
0
2
4
6
8
10
12
200
300
400
500
600
700
800
900

Figure 14.

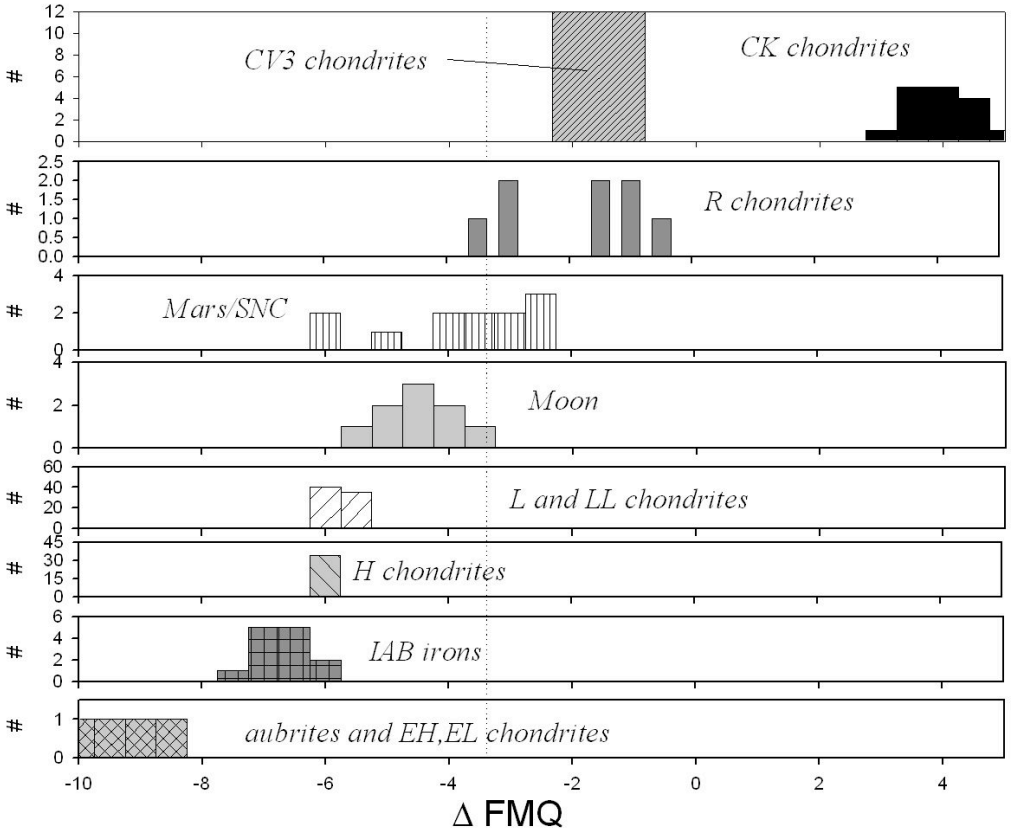
CV3 chondrites
CK chondrites
R chondrites
Mars/SNC
Moon
L and LL chondrites
H chondrites
IAB irons
aubrites and EH,EL chondrites
#
Δ FMQ

Figure 15.

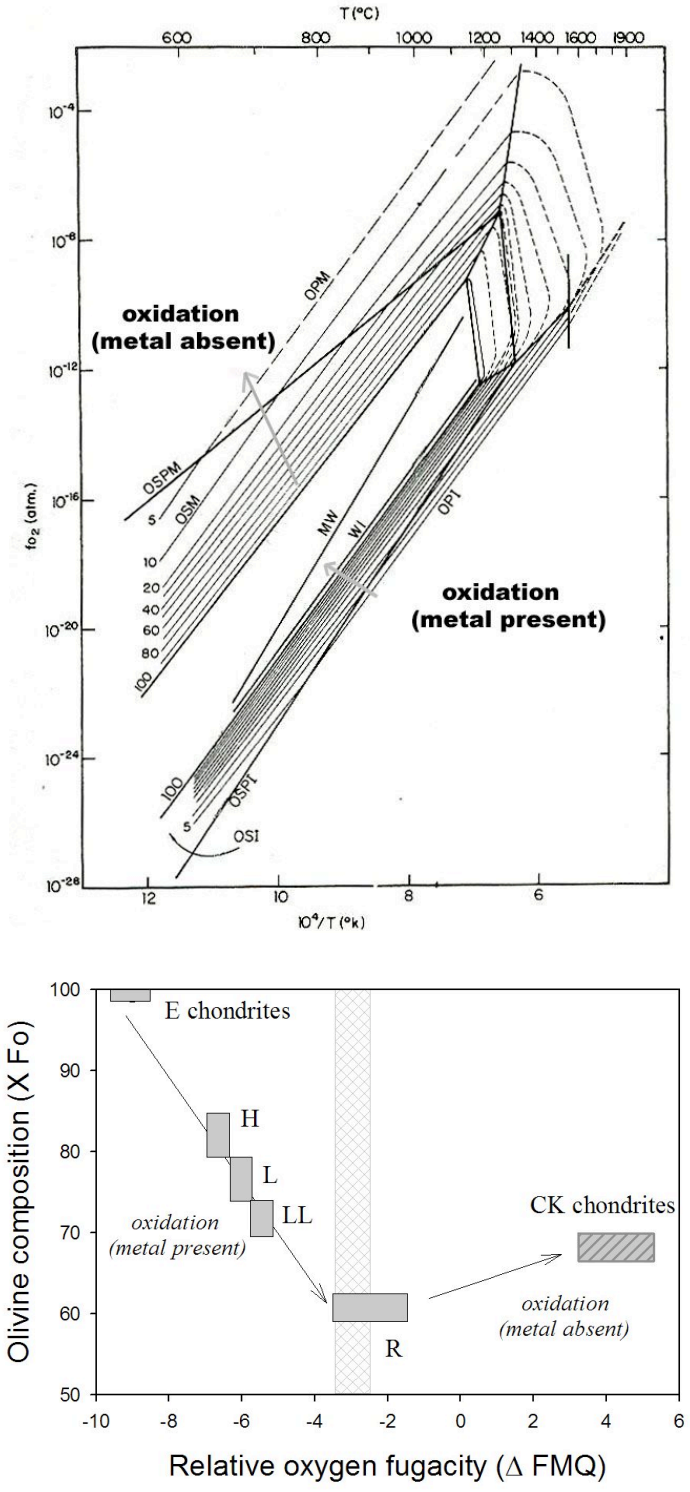
T(°C)
600
800
1000
1200
1400
1600
1900
oxidation
(metal absent)
oxidation
(metal present)
OPM
OSPM
OSM
MW
WI
OPT
OSPT
OSI
5
10
20
40
60
80
100
fo2 (atm.)
10⁴/T (°k)
12
10
8
6
E chondrites
H
L
LL
R
CK chondrites
oxidation
(metal present)
oxidation
(metal absent)
Olivine composition (X Fo)
Relative oxygen fugacity (Δ FMQ)

Figure 16.